16 March, 2001

OMV Australia Pty Ltd
Level 29, St Martins Tower
44 St Georges Tce
PERTH WA 6000

Attention: Tim Morison

FINAL REPORT: 0439-01
BASS STRAIT SAMPLES

CLIENT REFERENCE:	Purchase Order No. P2001-00052
MATERIAL:	Eight sidewall core samples
LOCALITY:	Bass Strait
WORK REQUIRED:	Petrology and reservoir quality

Please direct technical enquiries regarding this work to the signatory below under whose supervision the work was carried out.

PETER N CROZIER
Operations Manager

PETROLOGY

of

BASS STRAIT SAMPLES

for

OMV AUSTRALIA PTY LTD

by

ACS LABORATORIES PTY LTD

PETROLOGY

of

BASS STRAIT SAMPLES

A report prepared for

OMV AUSTRALIA PTY LTD

by

JULIAN C. BAKER Ph.D.

March 2001

C O N T E N T S

C O N T E N T S cont.

Page

FIGURES

APPENDICES

EXECUTIVE SUMMARY

A petrological study was carried out on eight, poor quality, impact-damaged sidewall core samples from Bass Strait. Analytical techniques used were thin-section analysis, bulk rock/clay fraction X-ray diffraction analysis and scanning electron microscopy.

The top three samples (817.1m, 818.7m, 822.0m) are poorly to moderately sorted, coarse to very coarse grained subarkoses and a quartzarenite, whereas the bottom five samples (835.7m, 837.9m, 843.0m, 850.7m, 889.1m) are moderately-well to well sorted, fine grained subarkoses. Argillaceous (mudrock, marl) fragments are included in the top two samples.

Framework grains are almost entirely granitic quartz and K-feldspar and also include mica, micaceous metasedimentary rock fragments, chert and accessory heavy minerals. Fine grained sandstones are more feldspathic than coarse to very coarse grained sandstones, and, unlike the coarser sandstones, contained abundant micaceous grains at the time of accumulation.

Detrital clay at 817.1m and 818.7m occurs mainly as a constituent of argillaceous fragments. Pyritic detrital clay matrix is common at 850.7m. Authigenic clay pseudomatrix that has formed by alteration of micaceous grains is abundant at 835.7m, 837.9m, 843.0m and 889.1m. Clay minerals are almost entirely illite and kaolinite and also include contaminant smectite.

Sandstone at 822.0m is extensively cemented by early-diagenetic marcasite (FeS_2), and sandstone at 850.7m is partly cemented by patchy, early-diagenetic pyrite.

The only other major diagenetic effect besides authigenic clay formation and iron sulphide cementation is the compactional deformation and dispersion of micaceous grains and authigenic clay to form pseudomatrix.

Original porosity characteristics of some samples (817.1m, 818.7m, 837.9m) have been almost totally eliminated by severe textural disruption caused by sidewall coring impact, hence data for these samples cannot be regarded as reliable. Porosity may be reduced in coarse grained sandstones at 817.1m and 818.7m by the presence of detrital clay matrix and authigenic clay pseudomatrix, but the extent of any such porosity reduction is impossible to determine due to poor sample quality. Intergranular porosity has been obliterated by marcasite cementation at 822.0m. Little visible porosity occurs at 850.7m due to the presence of detrital clay matrix and patchy pyrite cement, and little or no visible porosity occurs at 835.7m, 843.0m and 889.1m due to widespread pore filling by highly microporous, authigenic clay pseudomatrix. The sample from 837.9m has almost entirely disaggregated, but indications are that some pores were occupied by authigenic clay. If good macroporosity was present in any of the sands prior to sidewall coring, it has been obscured by impact-induced disaggregation and grain fragmentation.

High gamma ray readings between 835.7m and 843.0m reflect the presence of small amounts (0.3%) of radioactive heavy minerals (monazite, zircon).

1. INTRODUCTION

A petrological study was carried out on eight, poor quality, variably impact-damaged sidewall core samples from between 817.1m and 889.1m in a Bass Strait well (well name not supplied). The prime purpose of the study was to provide information on reservoir quality and also to determine the cause of high gamma ray readings below 822.0m. Sample depths and gamma ray values are given in Table 1.

TABLE 1. GAMMA RAY VALUES

Depth (m)	Approx. GR (api)
817.1	70
818.7	35
822.0	100
835.7	117
837.9	150
843.0	120
850.7	50
889.1	46

2. ANALYTICAL PROGRAM

2.1 Thin-Section Analysis

Thin-sections were cut in kerosene and impregnated with blue dyed epoxy resin to assist in porosity recognition. Mineral composition and visible porosity were determined by a count of 400 points in each thin-section, and mean grain size and sorting were estimated in thin-section with the aid of an eyepiece graticule. Monazite and zircon were counted together due to the difficulty of discriminating between these two minerals during point counting. Photomicrographs were taken to illustrate features such as composition, clay distribution and diagenetic effects.

2.2 X-Ray Diffraction Analysis

Qualitative, bulk rock X-ray diffraction (XRD) analysis was carried out on all samples using a finely ground whole rock powder sample. Qualitative XRD analysis was carried out on the fine fraction of all samples in order to precisely determine clay mineralogy. The fine fraction was separated from each sample by disaggregation and settling in distilled water and was air dried on glass discs to produce oriented specimens for XRD analysis. Samples were analysed in air dried condition and also following treatment with ethylene glycol.

2.3 Scanning Electron Microscopy

Scanning electron microscopy (SEM) was carried out on all samples to provide information on the nature and distribution of clays and the occurrence of radioactive heavy minerals. Back scattered electron imaging was used to locate heavy minerals. An energy dispersive spectrometer (EDS) attached to the SEM provided qualitative elemental data on heavy minerals and clays.

Texture and thin-section composition are given in Table 2, and QFR compositions are given in Table 3 and plotted in Figure 1. Bulk rock XRD analyses and clay mineralogy are given in Tables 4 and 5, respectively, and annotated XRD traces and photomicrographs are presented in Appendices 1 and 2, respectively.

Samples differ in terms of texture and composition. Consequently, samples are described individually rather than as a single suite.

3. SAMPLE DESCRIPTIONS

3.1 817.1m (Plates 1 & 2)

This sample consists mainly of loose, intact/broken, coarse sand- to granule-sized grains of granitic quartz and minor K-feldspar and also includes small (<3mm) fragments of sandy mudrock and impact-damaged (crushed), variably argillaceous, poorly to moderately sorted, medium to very coarse grained sandstone. Loose grains and sandstone fragments have a mean QFR composition that plots close to the quartzarenite-subarkose field boundary. Unbroken coarse quartz grains are mainly subrounded to rounded. K-feldspar is slightly to moderately altered orthoclase. One loose grain is a granitic rock fragment composed of intergrown orthoclase and polycrystalline quartz. Other detrital grains include rare intermediate volcanic rock fragments, accessory garnet and rare calcareous foram tests and fine muscovite that are associated with detrital clay. Radioactive heavy minerals (monazite, zircon) are absent.

Brown detrital clay is the main constituent of mudrock fragments and also forms dispersed matrix in the argillaceous sandstones. Clay minerals detected by XRD are kaolinite and illite. Widely scattered fine pyrite crystals/framboids are associated with the clay.

Original porosity characteristics of the sandstone have been obliterated by the effects of sidewall coring. Sandstone fragments are commonly crushed, but appear to have contained little intergranular porosity due to pore filling by dispersed detrital clay. Some loose quartz grains are partly enveloped by detrital clay, suggesting that these grains are derived from argillaceous lithologies. However, there is the possibility that loose quartz grains are also derived from clean sandstone that may have been partly macroporous.

TABLE 2. THIN-SECTION ANALYSES

Depth (m)	COMPOSITION																		TEXTURE	
	Qm	Qp	Cht	Kfe	Pla	GRF	MRF	SRF	Mca	M/Z	Tou	Sph	Mar	Py	FeS	AC	DC	VP	GS	Sorting
817.1	75.6	4.2	-	4.3	-	0.7	-	-	-	-	-	-	-	0.1	-	-	15.1	-	1.10	poor/mod
818.7	72.9	9.7	-	3.8	-	-	-	-	-	-	-	-	-	-	-	0.6	13.0	-	0.90	poor/mod
822.0	49.5	7.2	-	4.7	-	-	-	-	-	-	-	-	35.0	-	3.2	-	0.4	-	0.89	mod
835.7	75.8	0.5	0.3	7.8	-	-	-	-	0.8	0.3	-	0.3	-	0.5	-	13.7	-	-	0.16	mod-well
837.9	78.7	0.5	0.3	7.8	-	-	0.3	-	0.3	0.3	-	-	-	0.9	-	10.0	-	0.9	0.16	well
843.0	72.2	0.5	-	7.1	-	-	0.3	-	-	0.3	0.3	0.3	-	0.5	-	18.5	-	-	0.15	well
850.7	53.3	0.3	-	6.5	-	0.3	0.3	-	-	-	-	-	-	24.9	-	1.5	12.9	-	0.17	well
889.1	64.4	1.1	0.3	8.9	-	-	0.3	-	1.1	-	-	-	-	-	-	22.1	-	1.8	0.16	mod-well

Qm = monocrystalline quartz Qp = polycrystalline quartz Cht = chert Kfe = K-feldspar Pla = plagioclase GRF = granitic rock fragments MRF = metamorphic rock fragments SRF = sedimentary rock fragments Mca = mica M/Z = monazite/zircon Tou = tourmaline Sph = sphene Mar = marcasite (FeS_2) Py = pyrite FeS = unidentified marcasite decomposition product (possibly hydrated ferrous sulphate) AC = authigenic clay DC = detrital clay VP = visible porosity GS = estimated mean grain size (mm)

TABLE 3. QFR COMPOSITIONS

Depth (m)	Q Quartz + chert	F Feldspar	R Rock fragments
817.1	94.1	5.1	0.8
818.7	95.6	4.4	0.0
822.0	92.3	7.7	0.0
835.7	90.8	9.2	0.0
837.9	90.8	8.9	0.3
843.0	90.7	8.9	0.4
850.7	88.3	10.7	1.0
889.1	87.7	11.9	0.4

FIGURE 1. QFR COMPOSITIONS

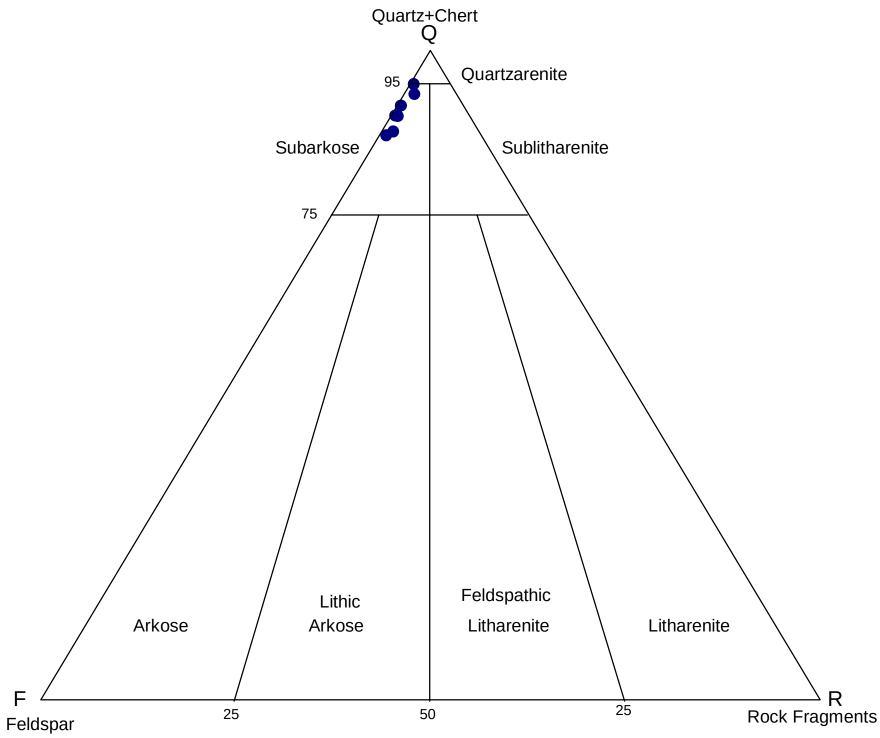

TABLE 4. BULK ROCK XRD ANALYSES

Depth (m)	Qtz	Kfe	I	K	Cal	Mar	Py	FeS	BaS	Gyp
817.1	A	m	T	-	-	-	-	-	-	-
818.7	A	m	T	T	T	-	-	-	-	-
822.0	A	m	-	-	-	M	-	m	-	-
835.7	A	m	m	m	-	-	-	-	m	-
837.9	A	m	m	m	-	-	-	-	-	-
843.0	A	m	m	m	-	-	-	-	-	-
850.7	A	m	m	m	-	-	m	-	-	m
889.1	A	m	m	m	-	-	-	-	-	-

Qtz = quartz Kfe = K-feldspar I = illite/mica K = kaolinite Cal = calcite Mar = marcasite (FeS_2)
Py = pyrite FeS = marcasite decomposition product (possibly hydrated ferrous sulphate) BaS = barite (contaminant) Gyp = gypsum (contaminant)

A = abundant (nominally >40%) M = major (10-40%) m = minor (1-10%) T = trace (<1%)

TABLE 5. CLAY MINERALOGY

Depth (m)	K	I	I/S	Sm	Chl
817.1	T	T	-	-	-
818.7	T	T	-	T	-
822.0	-	-	-	-	-
835.7	M	A	-	T	-
837.9	A	A	-	-	-
843.0	A	A	-	m	-
850.7	A	A	-	-	-
889.1	A	A	-	-	-

K = kaolinite I = illite/mica I/S = mixed-layer illite/smectite
Sm = smectite Chl = chlorite

A = abundant M = major m = minor T = trace

3.2 818.7m (Plates 3 & 4)

This sample is similar to the previous sample except that it has a higher proportion of sandstone fragments, all of which are severely crushed and/or partly disaggregated as a result of sidewall coring. Sandstone fragments are mainly poorly to moderately sorted and medium to very coarse grained, and are composed almost entirely of granitic quartz and minor K-feldspar (slightly to moderately altered orthoclase and microcline) as well as variable amounts of brown detrital clay and/or greenish illitic clay pseudomatrix. Illitic clay pseudomatrix appears to be an alteration product of mica. A single silt-sized monazite grain is included in one sandstone fragment. Clay minerals detected by XRD are kaolinite, illite and smectite. Other components of the sample besides sandstone fragments include loose, medium sand- to granule-sized grains of quartz and K-feldspar as well as fragments of barite-bearing drilling mud and marly mudrock composed mainly of brown clay that, in some fragments, supports ?mobilised, coarse to very coarse sand-sized grains of quartz and K-feldspar. Calcareous foram tests, fine calcareous shell fragments, fine muscovite and fine pyrite crystals are commonly associated with clay. One argillaceous fragment contains a 0.6mm siderite microconcretion, and there are rare radiating gypsum crystals that precipitated subsequent to coring.

Original porosity characteristics of the cleaner sandstone fragments have been obliterated by the effects of severe impact damage. Accordingly, it is impossible to determine whether these sandstone fragments originally contained intergranular porosity. Pores in some sandstone fragments appear to have been occupied by detrital clay matrix and authigenic clay pseudomatrix.

3.3 822.0m (Plates 5 & 6)

Framework grains in this severely fractured, but mainly intact, massive, moderately sorted, coarse grained subarkose are mainly granitic quartz and minor K-feldspar (orthoclase, microcline) and also include granitic rock fragments (intergrown quartz, K-feldspar and muscovite), low grade metasedimentary rock fragments (meta-argillite) and altered muscovite. Quartz grains are mainly subangular to rounded. Radioactive heavy minerals are absent.

Most intergranular spaces are filled by early diagenetic marcasite (FeS_2) that has decomposed in some areas to form an unidentified, finely-crystalline mineral (possibly hydrated ferrous sulphate) that rims framework grains and fills intragranular fractures. The unidentified mineral also partly rims the sample periphery, indicating that the mineral formed subsequent to coring. Marcasite not only occupies intergranular spaces, but also fills microfractures within quartz grains. Framework grains are commonly supported by marcasite cement.

Although rare detrital clay matrix occupies intergranular spaces, no clay minerals were detected by XRD.

Ignoring artificial fracture porosity that is the result of sidewall coring, the sample lacks macroporosity due to the presence of abundant marcasite cement. Permeability would be negligible.

3.4 835.7m (Plates 7 & 8)

This sample is an intact, massive, moderately-well sorted, fine grained subarkose in which framework grains are mainly quartz and subordinate K-feldspar and also include muscovite, biotite, micaceous metasedimentary rock fragments, chert and accessory heavy minerals. Quartz is mainly angular to subangular. K-feldspar is fresh to slightly altered orthoclase and microcline. Quartz and feldspar grains are locally fractured and crushed due to sidewall coring. Mica, which was originally abundant in the sample as discrete grains and as a constituent of micaceous metasedimentary rock fragments, has partly to completely decomposed to illite and kaolinite that have compactionally dispersed to form pervasive pseudomatrix. Accessory heavy minerals are monazite, zircon, tourmaline, sphene, Fe-Ti oxides, and leucoxene. Radioactive heavy minerals (monazite, zircon) are widely scattered, but are sufficiently common (0.3%) to have been recorded during point counting. No monazite and zircon were located in the sample split used for SEM analysis.

Concentrations of fine pyrite crystals replace altered biotite and rare detrital clay. Other opaques besides pyrite include leucoxene that has formed by alteration of detrital Fe-Ti oxides and sphene.

Clay is mainly authigenic illite and kaolinite that have formed by decomposition of micaceous grains. Most micaceous grains are partly altered to illite and/or kaolinite, and illitic remnants of precursor mica commonly occur within authigenic kaolinite. XRD analyses indicate that the clay mineral suite is dominated by illite and subordinate kaolinite and also includes trace smectite.

The main diagenetic effects are mica alteration to clay, and mica/authigenic clay compaction to form pervasive pseudomatrix.

The sandstone is totally microporous due to the presence of finely dispersed, authigenic clay pseudomatrix, and thus would have low permeability, especially given the fine grain size.

3.5 837.9m (Plates 9 & 10)

This largely disaggregated, well sorted, fine grained subarkose has a framework grain composition identical to the previous sample. The sample consists mainly of loose grains and also includes small, intact sandstone fragments up to 8mm long in which all intergranular areas are filled by dispersed brown detrital clay matrix and/or kaolinitic/illitic pseudomatrix that is similar to that in the previous sample. The sample also includes a contaminant fragment of foraminiferal marl. Clay minerals detected by XRD are kaolinite and illite. Monazite and zircon grains are widely scattered, but are sufficiently common (0.3%) to have been recorded during point counting. No monazite and zircon were located in the sample split used for SEM analysis.

Diagenetic effects include mica alteration to illite and kaolinite, mica/authigenic clay compaction to form pseudomatrix, and localised precipitation of fine pyrite.

Original porosity characteristics have been almost totally obliterated by impact-induced disaggregation. Authigenic clay is attached to some loose grains, and between loose grains there is mobilised authigenic clay and fine mica, indicating that loose grains are derived from a sandstone in which there was some porosity reduction by authigenic clay formation and compaction. This is consistent with the fact that the sample includes small intact sandstone fragments in which intergranular spaces are filled by illitic/kaolinitic pseudomatrix and detrital clay matrix. The recorded visible porosity value of 0.9% can only be regarded as speculative, but indications are that at least some of the sample was originally not highly macroporous due to pore filling by clay.

3.6 843.0m (Plates 11 & 12)

Most of this sample is made up of large (up to 2cm) fragments of well sorted, fine grained subarkose that has the same framework grain composition as the previous fine grained sandstones. Loose grains and mobilised authigenic clay are also common. Although sandstone fragments are intact, constituent grains are locally fractured and crushed as a result of sidewall coring impact. In all sandstone fragments, intergranular areas are completely filled by patchy detrital clay matrix and widespread kaolinitic/illitic pseudomatrix that has formed by alteration of micaceous grains. Clay minerals detected by XRD are kaolinite, illite and minor smectite. Monazite and zircon grains are widely scattered, but are sufficiently common (0.3%) to have been recorded during point counting. No monazite and zircon were located in the sample split used for SEM analysis.

Diagenetic effects are the same as in the previous sample.

Sandstone fragments are totally microporous due to extensive pore filling by authigenic clay pseudomatrix and subordinate detrital clay matrix. Coexisting loose grains are the disaggregated remains of microporous, low permeability sandstone.

3.7 850.7m (Plates 13 & 14)

This sample is a fragmented/partly disaggregated, argillaceous, well sorted, fine grained subarkose with the same framework grain composition as the previous fine grained sandstones. A large (1 cm) intact sandstone fragment is extensively cemented by pyrite that has replaced detrital clay matrix. Other intact sandstone fragments contain abundant brown detrital clay matrix in which there is finely disseminated pyrite crystals, scattered pyrite microconcretions and small patches of pyrite cement. The pyrite has decomposed (subsequent to coring) in some areas to form a fracture-filling, finely-crystalline mineral that appears similar to the unidentified mineral (possibly hydrated ferrous sulphate) that is associated with marcasite at 822.0m. Clay minerals detected by XRD are kaolinite and illite, which, unlike in the previous fine grained sandstones, mainly have a detrital rather than authigenic origin. Framework grains are commonly supported by detrital clay matrix and pyrite cement. Accessory heavy minerals include monazite, zircon and tourmaline. Monazite and zircon grains are far less common than in the previous fine grained sandstones, and were not located in the sample split used for SEM analysis.

Diagenetic effects include replacement of detrital clay by early-diagenetic pyrite cement, and alteration of micaceous grains to illite and kaolinite.

Ignoring artificial porosity resulting from impact-induced fracturing and disaggregation, the sample contains little intergranular porosity due to extensive pore filling by detrital clay and pyrite cement. Permeability would be very low.

3.8 889.1m (Plates 15 & 16)

This fragmented subarkose is very similar to the sample from 843.0m, except that it is moderately-well sorted rather than well sorted and includes small, localised areas in which intergranular spaces between loosely packed framework grains are largely free of authigenic clay. Minor (1.8%) visible porosity is accounted for by primary intergranular pores that are preserved in these areas. Elsewhere, intergranular spaces are completely filled by authigenic illite and kaolinite pseudomatrix that has formed by alteration of micaceous grains, which were evidently abundant in the sample at the time of accumulation. Clay minerals detected by XRD are kaolinite and illite. Monazite and zircon content is less than 0.01%, with only four or five monazite/zircon grains occurring in the thin-section. No monazite and zircon were located in the sample split used for SEM analysis.

Diagenetic effects include mica alteration to illite and kaolinite, mica/authigenic clay compaction, and localised precipitation of fine pyrite.

The sandstone is almost totally microporous due to extensive pore filling by authigenic clay pseudomatrix. Primary intergranular pores are confined to localised areas and thus would not be conducive to permeability.

4. CAUSE OF HIGH GAMMA RAY READINGS

The three sandstones from between 835.7m and 843.0m have gamma ray values (117-150 API gamma units) that are much higher than gamma ray values for the other samples (35-100 api gamma units) (Table 1). Unlike the other samples, these three sandstones, all of which are fine grained, contain radioactive heavy mineral grains (monazite, zircon) that, although widely scattered, are sufficiently common (0.3%) to have registered in the point count analyses. The correspondence between very high gamma ray values and elevated contents of monazite and zircon grains is taken to indicate that the high gamma ray values are a response to the presence of these radioactive grains.

5. SUMMARY AND CONCLUSIONS

- Eight, poor quality, variably impact-damaged sidewall core samples from Bass Strait are poorly to moderately sorted, coarse to very coarse grained subarkoses and a quartzarenite (817.1 - 822.0m) and moderately-well to well sorted, fine grained subarkoses (835.7 - 889.1m). Framework grains are almost entirely granitic quartz and K-feldspar and, particularly in the fine grained sandstones, also include mica (muscovite, biotite), micaceous metasedimentary rock fragments, chert and accessory heavy minerals (monazite, tourmaline, sphene, zircon, leucoxene, Fe-Ti oxides, garnet). Fine grained sandstones are more feldspathic than coarse to very coarse grained sandstones, and, unlike the coarser sandstones, contained abundant micaceous grains at the time of accumulation.

- Detrital clay at 817.1m and 818.7m occurs mainly as a constituent of argillaceous (mudrock/marl) fragments. Detrital clay matrix is common at 850.7m. Sandstones from 835.7m, 837.9m, 843.0m and 889.1m contain abundant authigenic clay that has formed by alteration of micaceous grains. Detrital and authigenic clay minerals are illite and kaolinite. Smectite, which was only detected in three samples, is probably a contaminant.

- The sandstone from 822.0m is extensively cemented by early-diagenetic marcasite (FeS_2), and the sandstone from 850.7m is partly cemented by patchy, early-diagenetic pyrite. The other sandstones are virtually uncemented.

- The only other major diagenetic effect besides authigenic clay formation and iron sulphide cementation is the compactional deformation and dispersion of micaceous grains and authigenic clay to form widespread pseudomatrix (mainly in samples from 835.7m, 843.0m and 889.1m).

- Original porosity characteristics of some samples (817.1m, 818.7m, 837.9m) have been almost totally obscured by severe textural disruption caused by sidewall coring impact. Porosity may be reduced in coarse grained sandstones at 817.1m and 818.7m by the presence of detrital clay and authigenic clay pseudomatrix, but the extent of any such porosity reduction is impossible to determine due to poor sample quality. The coarse grained sandstone from 822.0m lacks visible porosity on account of being strongly cemented by marcasite. Little visible porosity occurs in the fine grained sandstone from 850.7m due to pore filling by detrital clay matrix and patchy pyrite cement, and little or no visible porosity occurs at 835.7m, 843.0m and 889.1m due to widespread pore filling by highly microporous, authigenic clay pseudomatrix. The sample from 837.9m has almost entirely disaggregated, but indications are that at least some pores were filled by authigenic clay.

- Permeability would be low (<10-15md) at 822.0m, 835.7m, 843.0m, 850.7m and 889.1m due to the presence of iron sulphide cement (822.0m, 850.7m) and pore-filling clay. The degree to which permeability is reduced by pore-filling clay at 817.1m, 818.7m and 837.9m cannot be determined due to poor sample quality.

- High gamma ray readings between 835.7m and 843.0m reflect the presence of small amounts (0.3%) of radioactive heavy minerals (monazite, zircon).

APPENDIX 1

XRD TRACES

Key to abbreviations:

Ba	=	barite (contaminant)
Ca	=	calcite
Gy	=	gypsum (contaminant)
I	=	illite
K	=	kaolinite
KF	=	K-feldspar
M	=	marcasite
Py	=	pyrite
Q	=	quartz
S	=	siderite
?	=	?hydrated ferrous sulphate

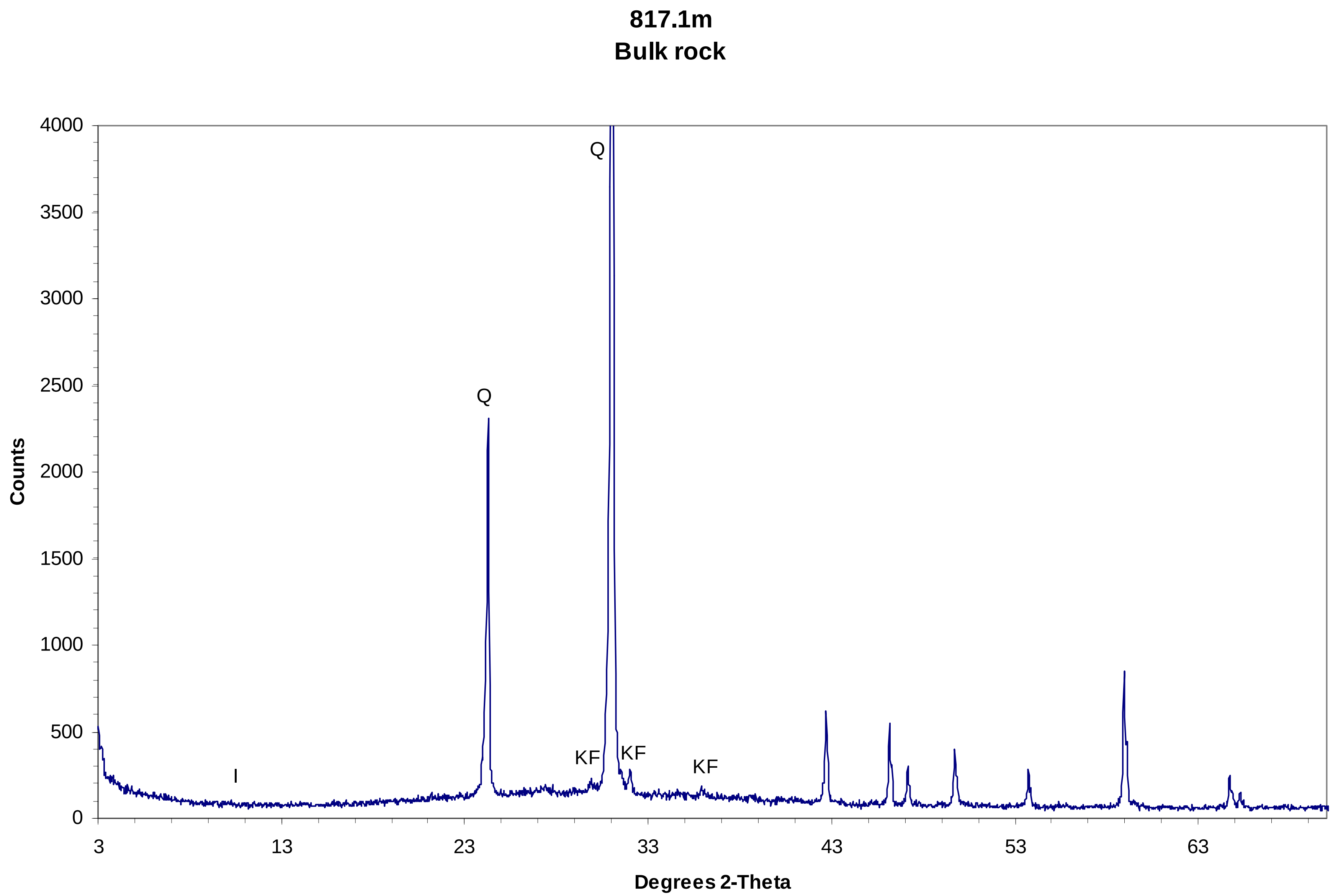
817.1m
Bulk rock
Counts
Degrees 2-Theta
Q
Q
KF
KF
KF
I
0
500
1000
1500
2000
2500
3000
3500
4000
3
13
23
33
43
53
63

817.1m
Fine fraction

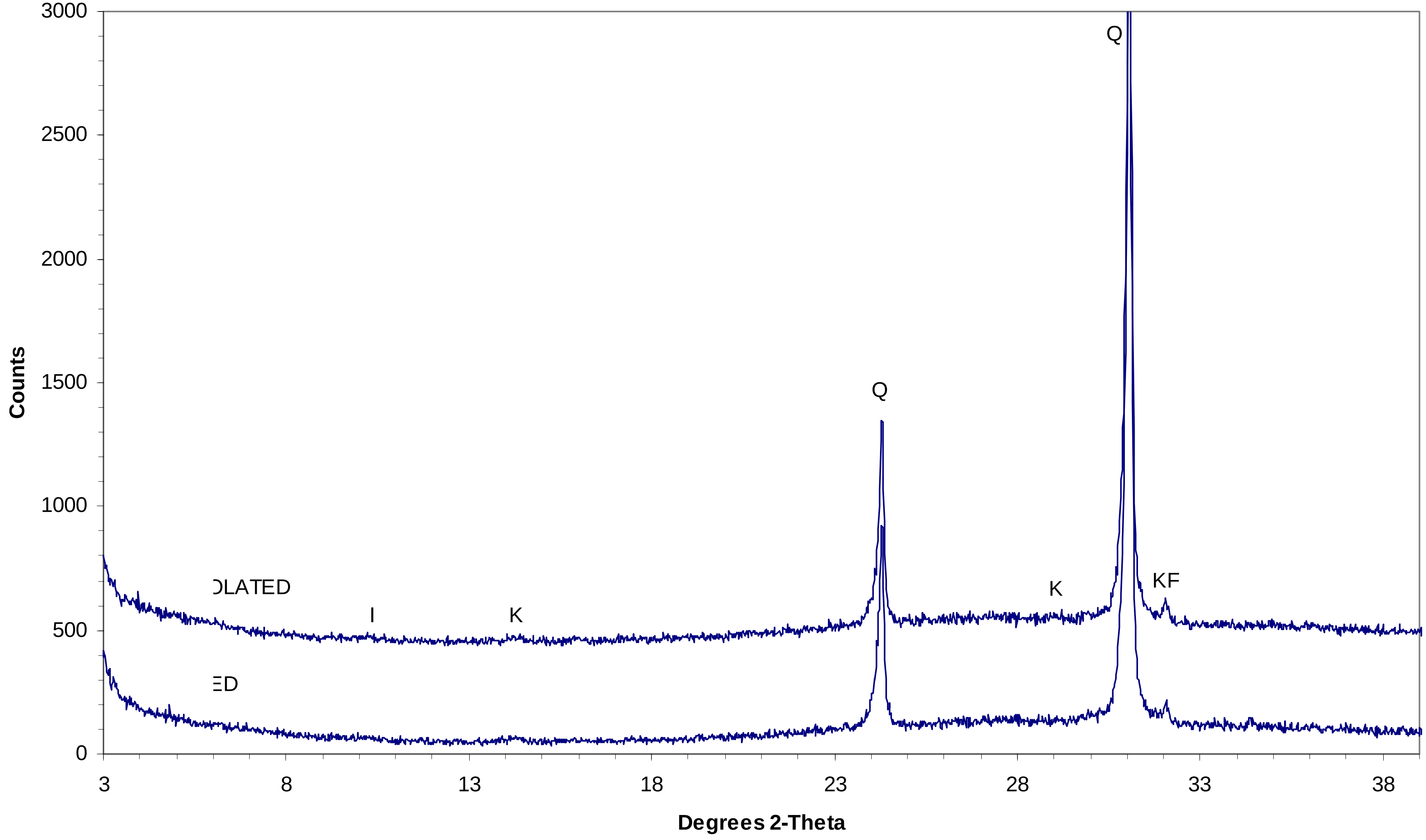

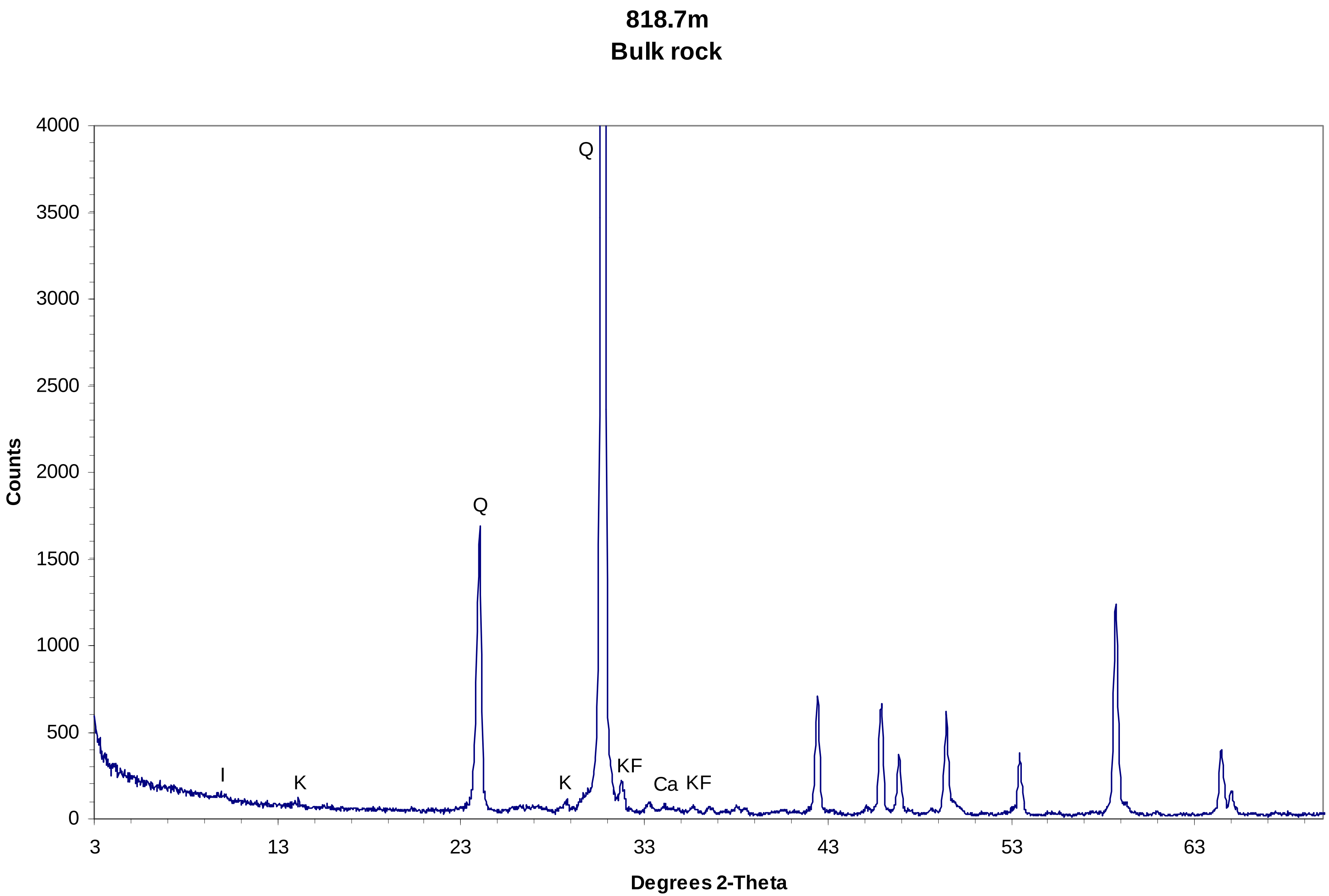
818.7m
Bulk rock
Counts
Degrees 2-Theta
0
500
1000
1500
2000
2500
3000
3500
4000
3
13
23
33
43
53
63
Q
Q
I
K
K
KF
Ca
KF

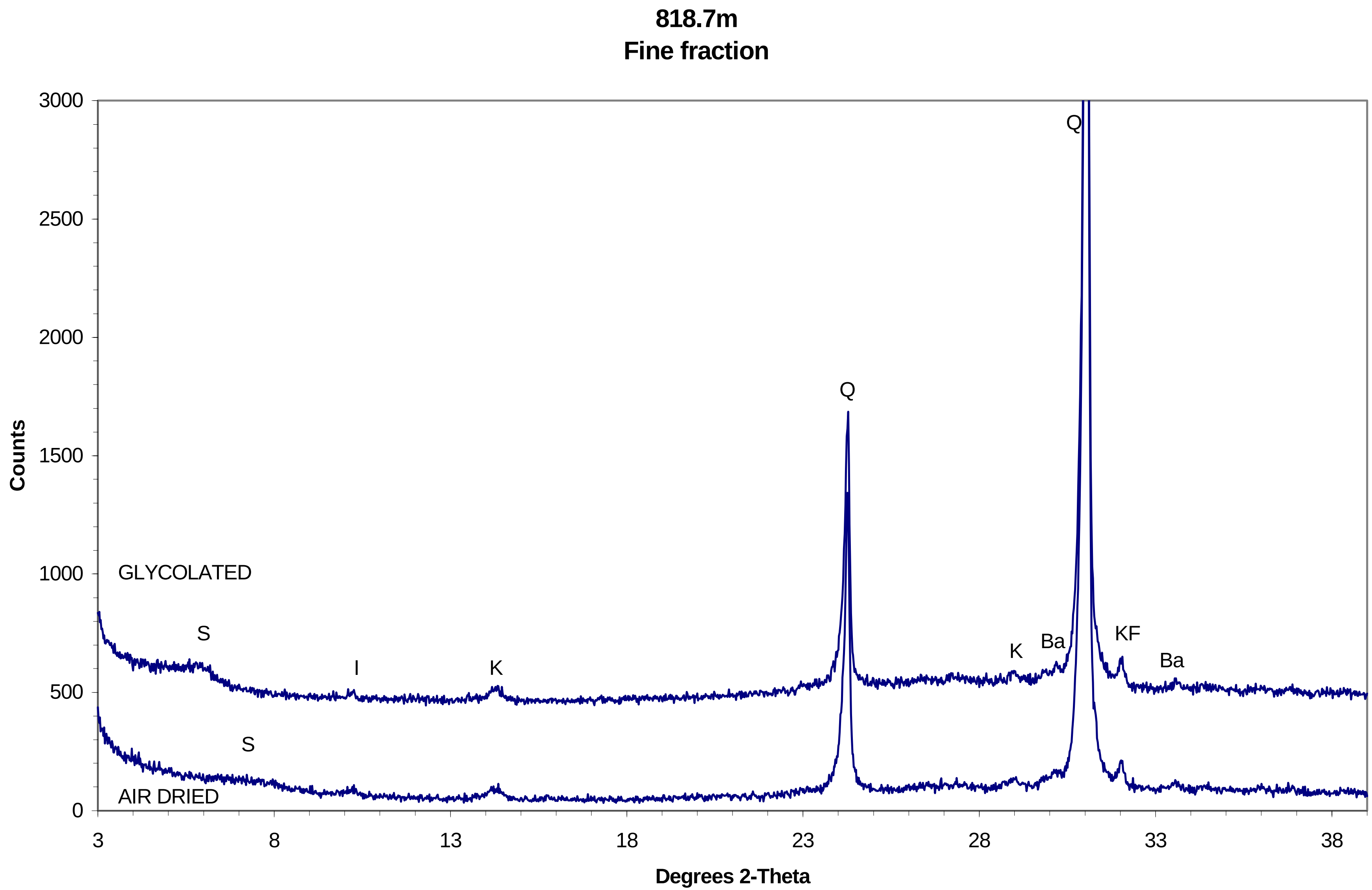

818.7m
Fine fraction
Counts
Degrees 2-Theta
3000
2500
2000
1500
1000
500
0
3
8
13
18
23
28
33
38
GLYCOLATED
AIR DRIED
S
I
K
Q
K
Ba
Q
KF
Ba
S

822.0m
Bulk rock

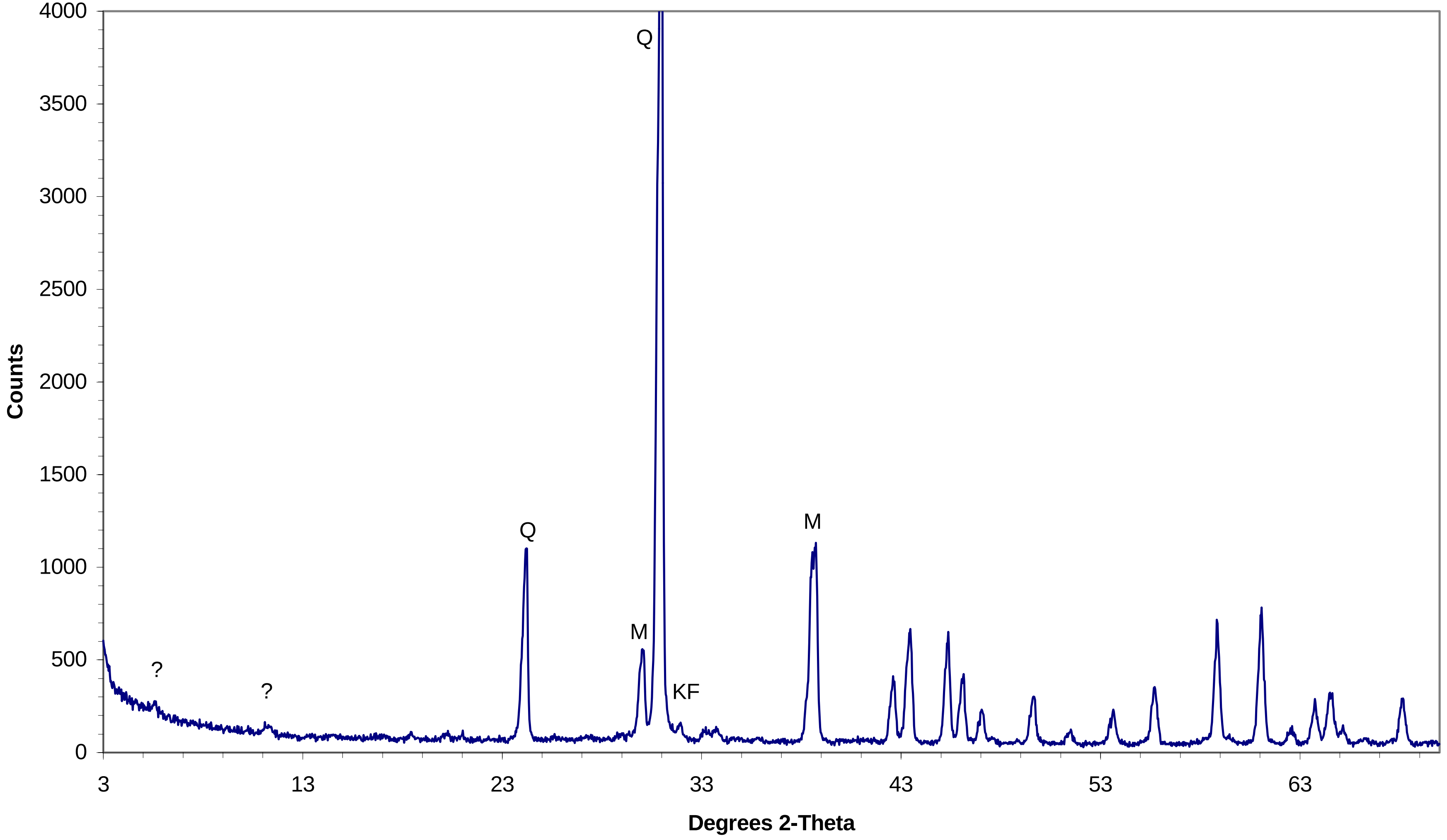

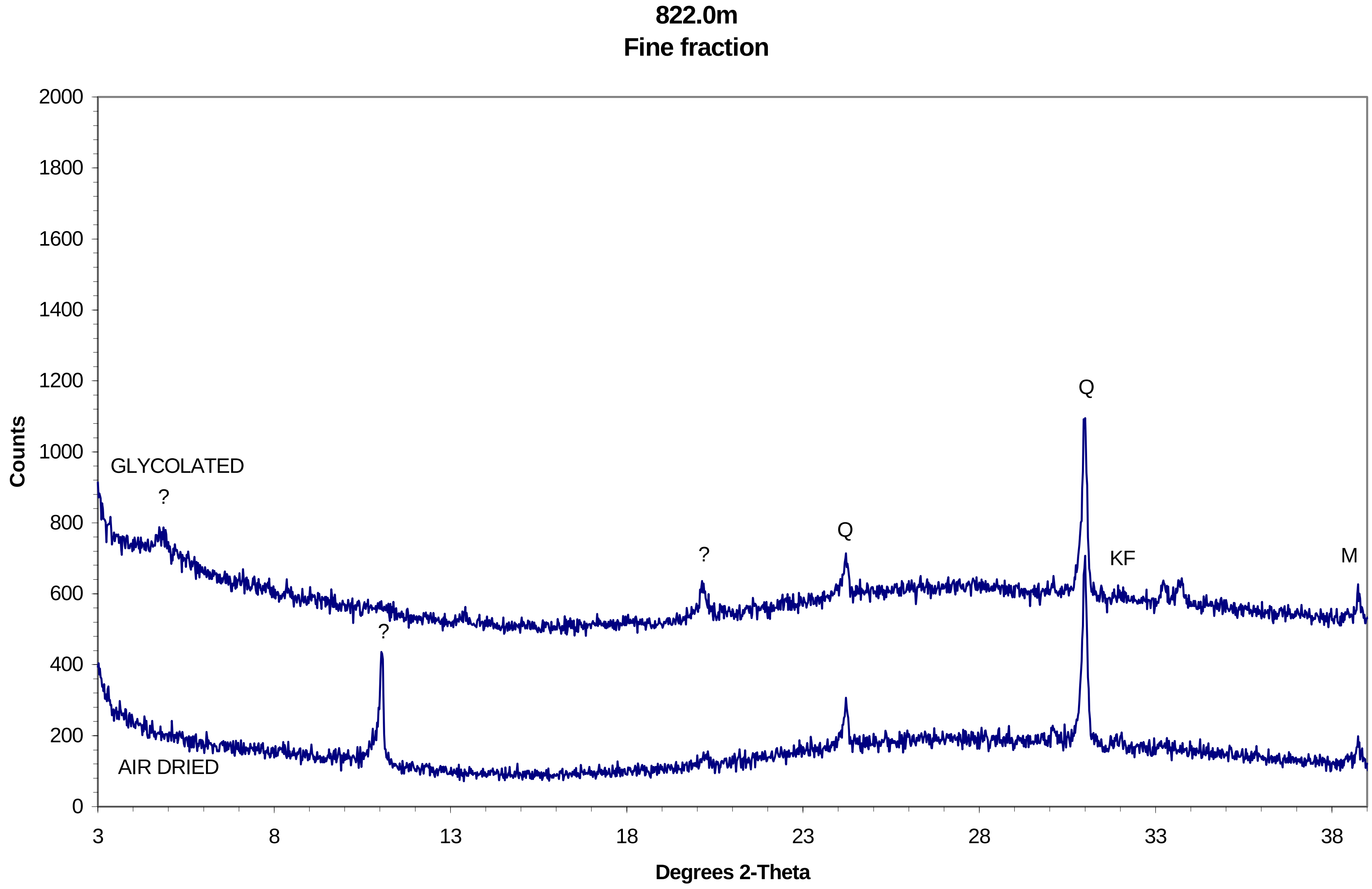
822.0m
Fine fraction
Counts
2000
1800
1600
1400
1200
1000
800
600
400
200
0
GLYCOLATED
?
?
Q
Q
KF
M
?
AIR DRIED
3
8
13
18
23
28
33
38
Degrees 2-Theta

835.7m
Bulk rock

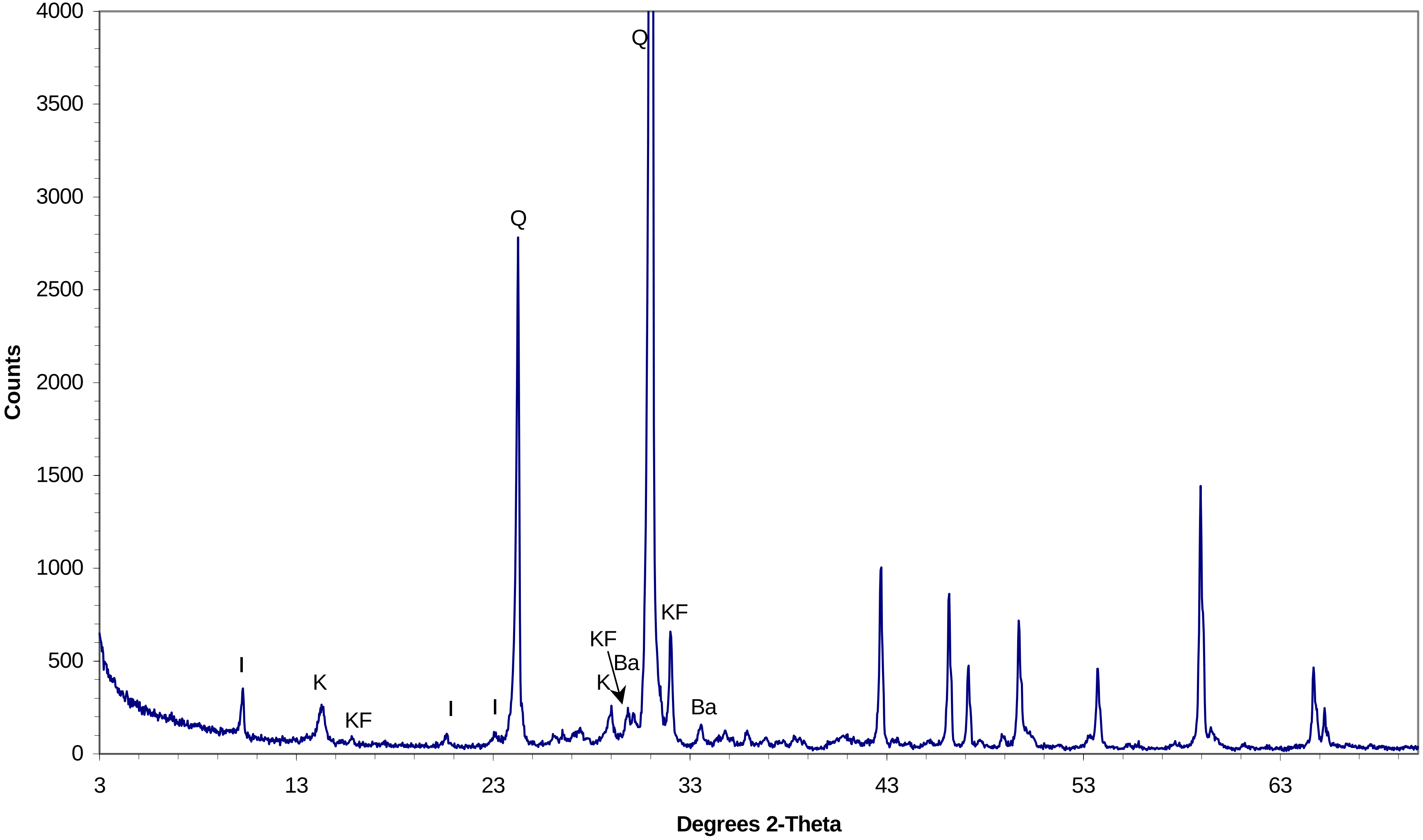

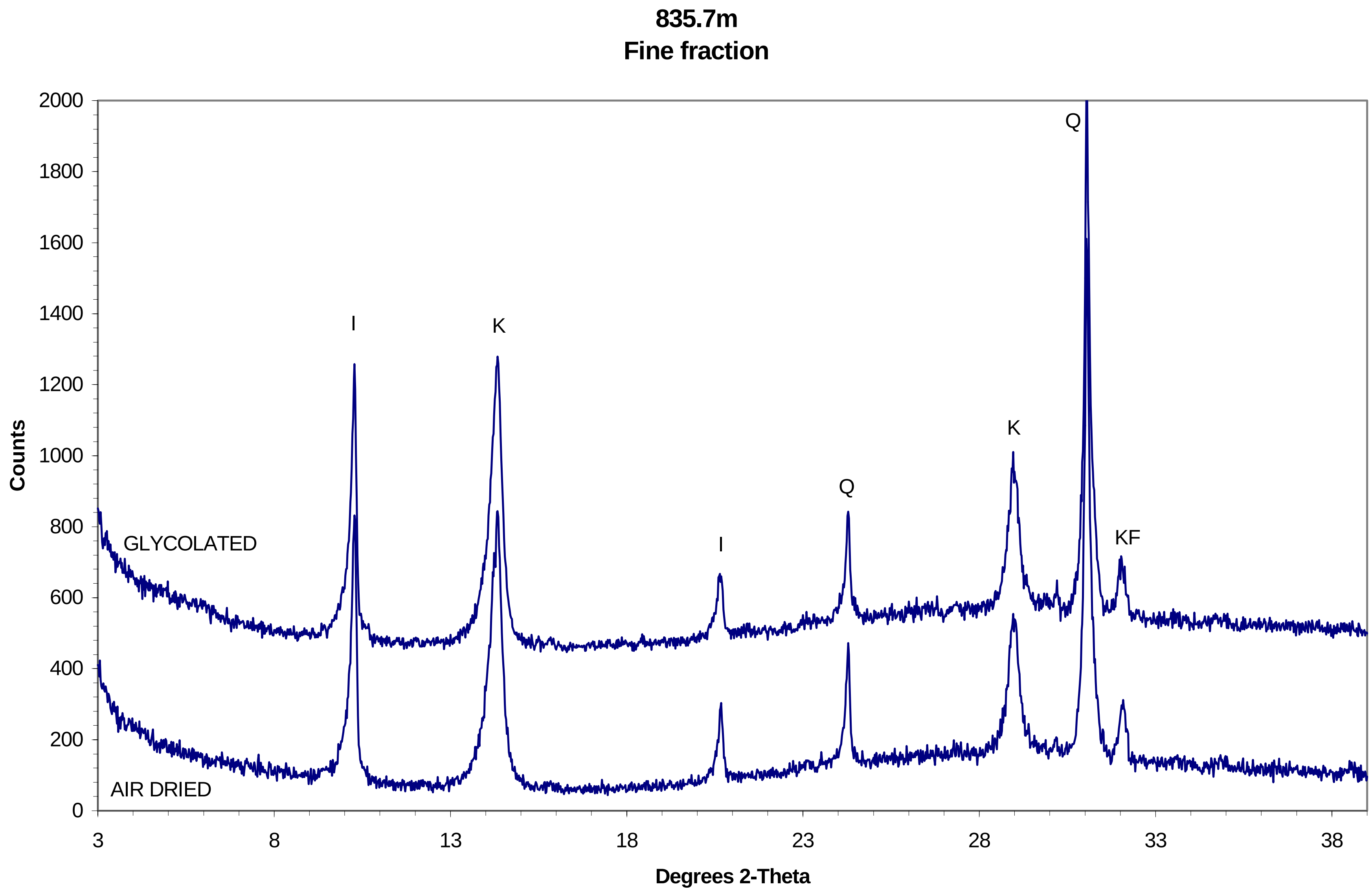
835.7m
Fine fraction
Counts
Degrees 2-Theta
GLYCOLATED
AIR DRIED
I
K
I
Q
K
Q
KF
0
200
400
600
800
1000
1200
1400
1600
1800
2000
3
8
13
18
23
28
33
38

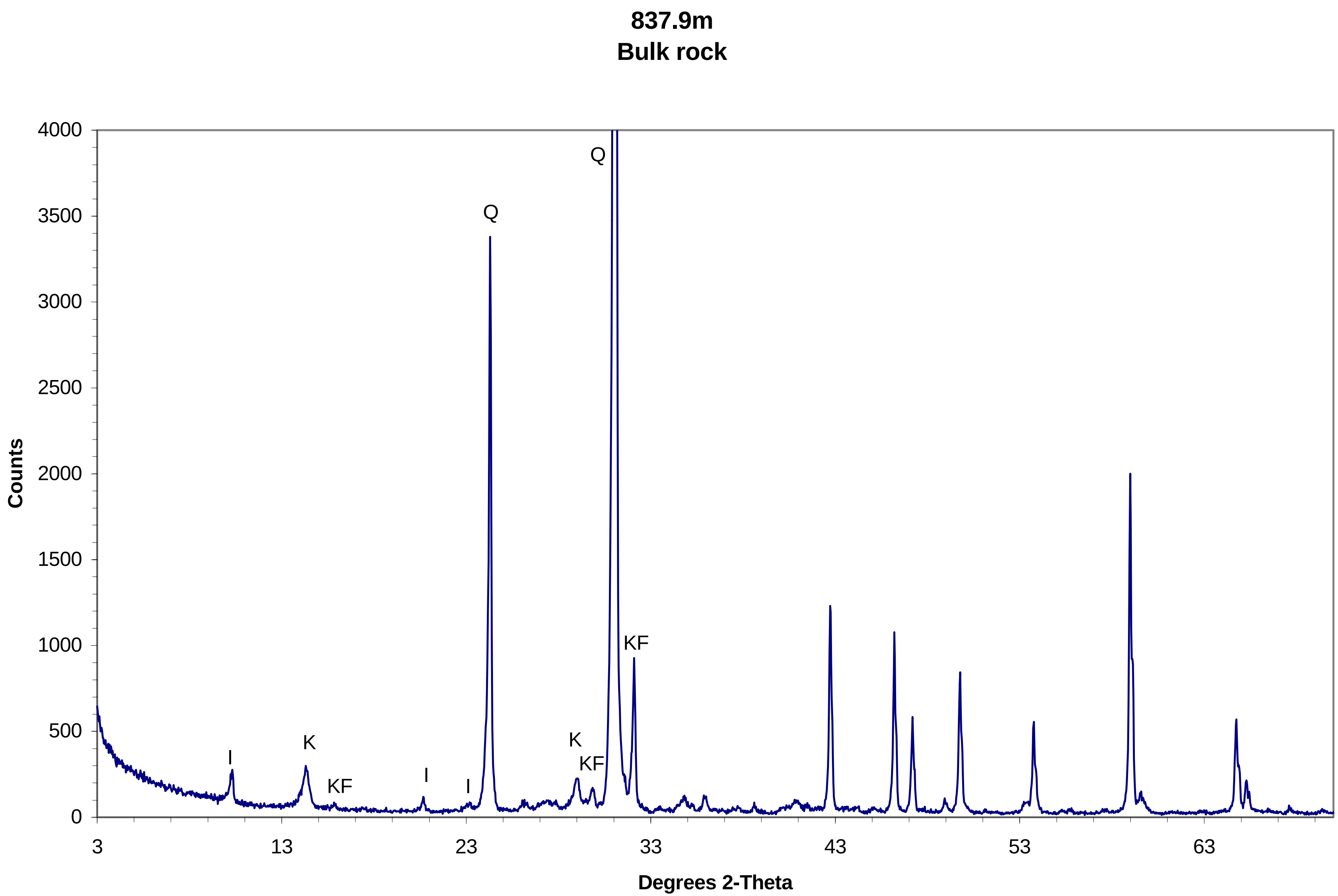
837.9m
Bulk rock
Counts
Degrees 2-Theta
4000
3500
3000
2500
2000
1500
1000
500
0
3
13
23
33
43
53
63
Q
Q
KF
I
K
KF
I
I
K
KF

837.9m
Fine fraction

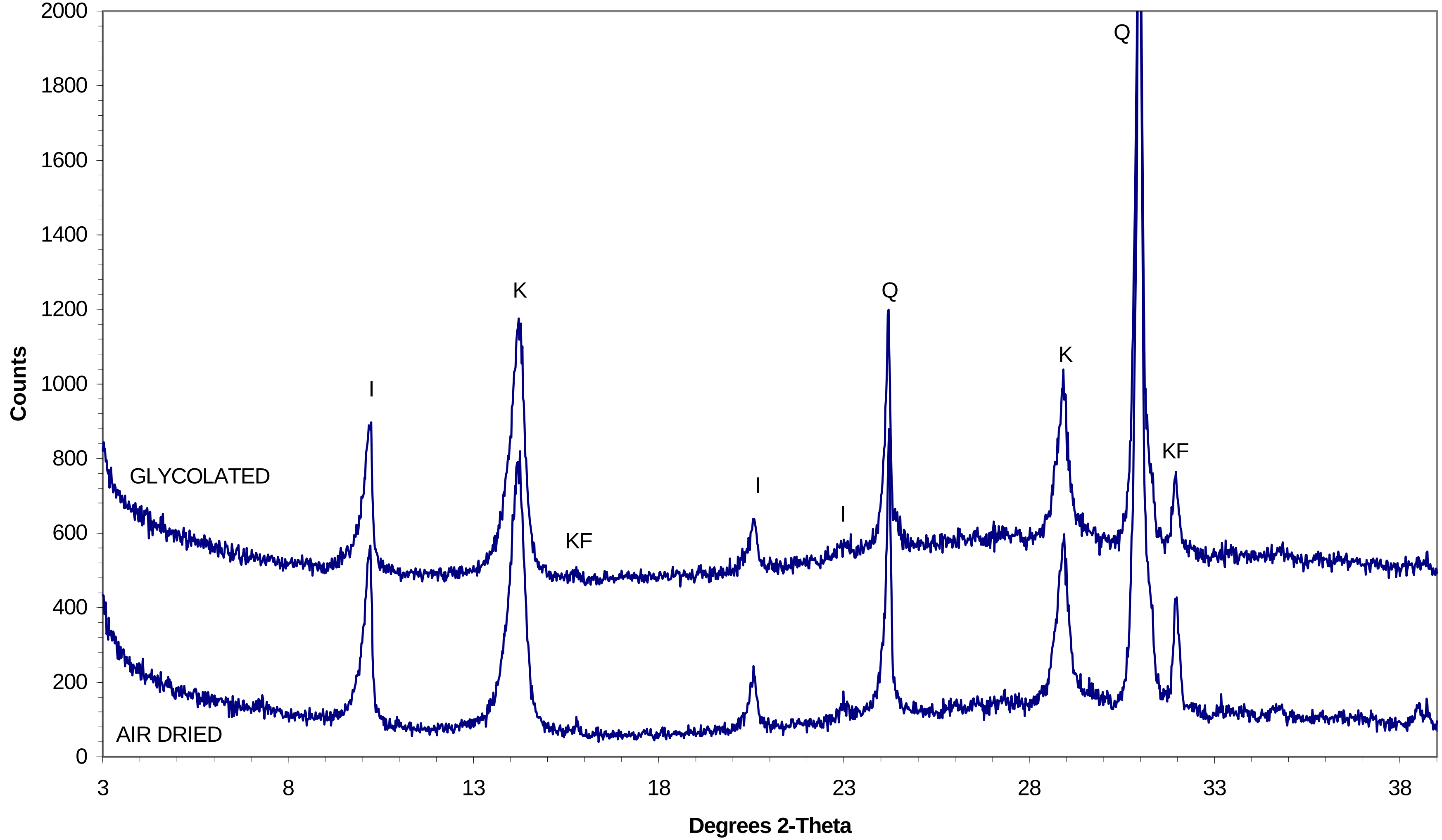

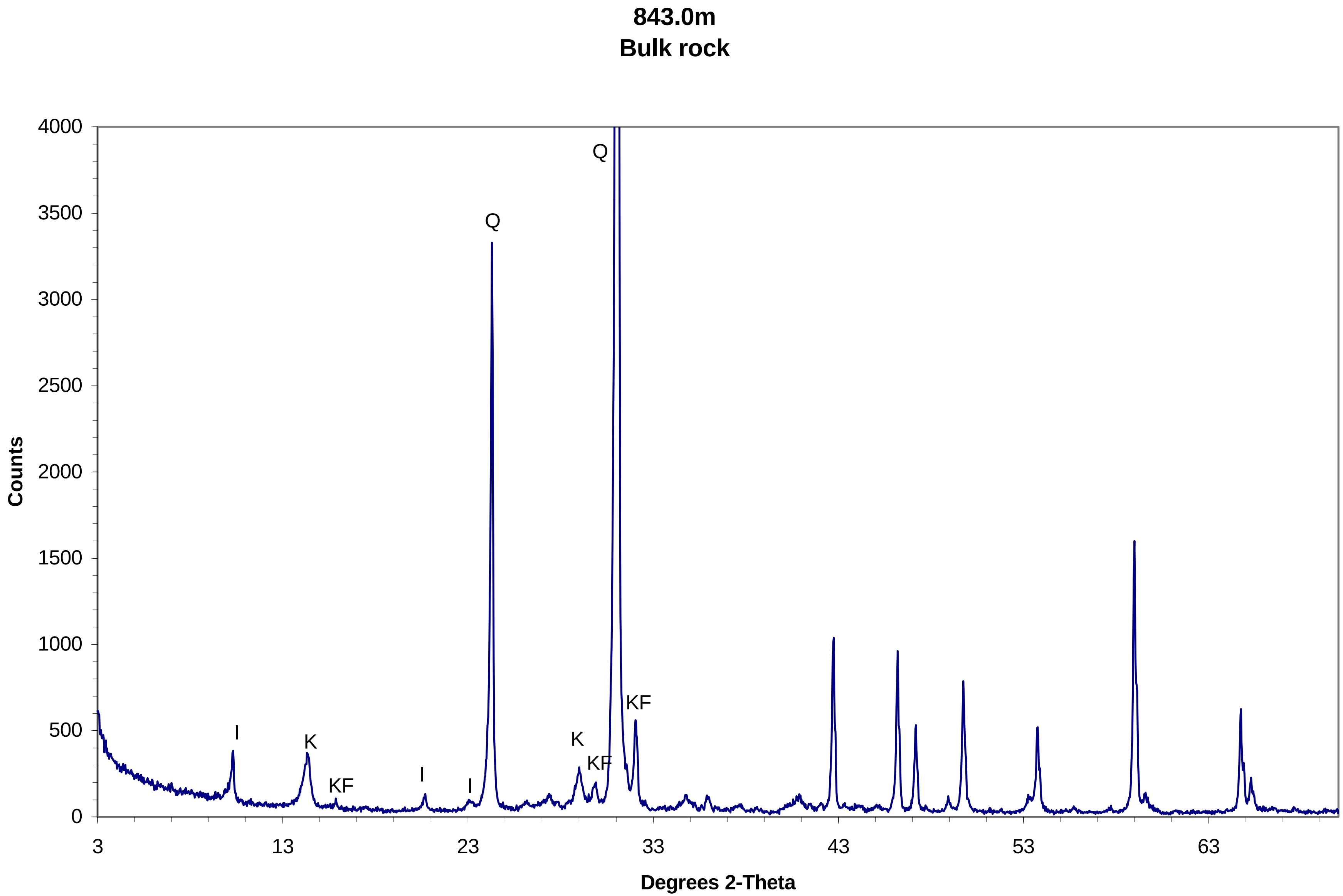
843.0m
Bulk rock
Counts
4000
3500
3000
2500
2000
1500
1000
500
0
3
13
23
33
43
53
63
Degrees 2-Theta
Q
Q
I
K
KF
I
I
K
KF
KF

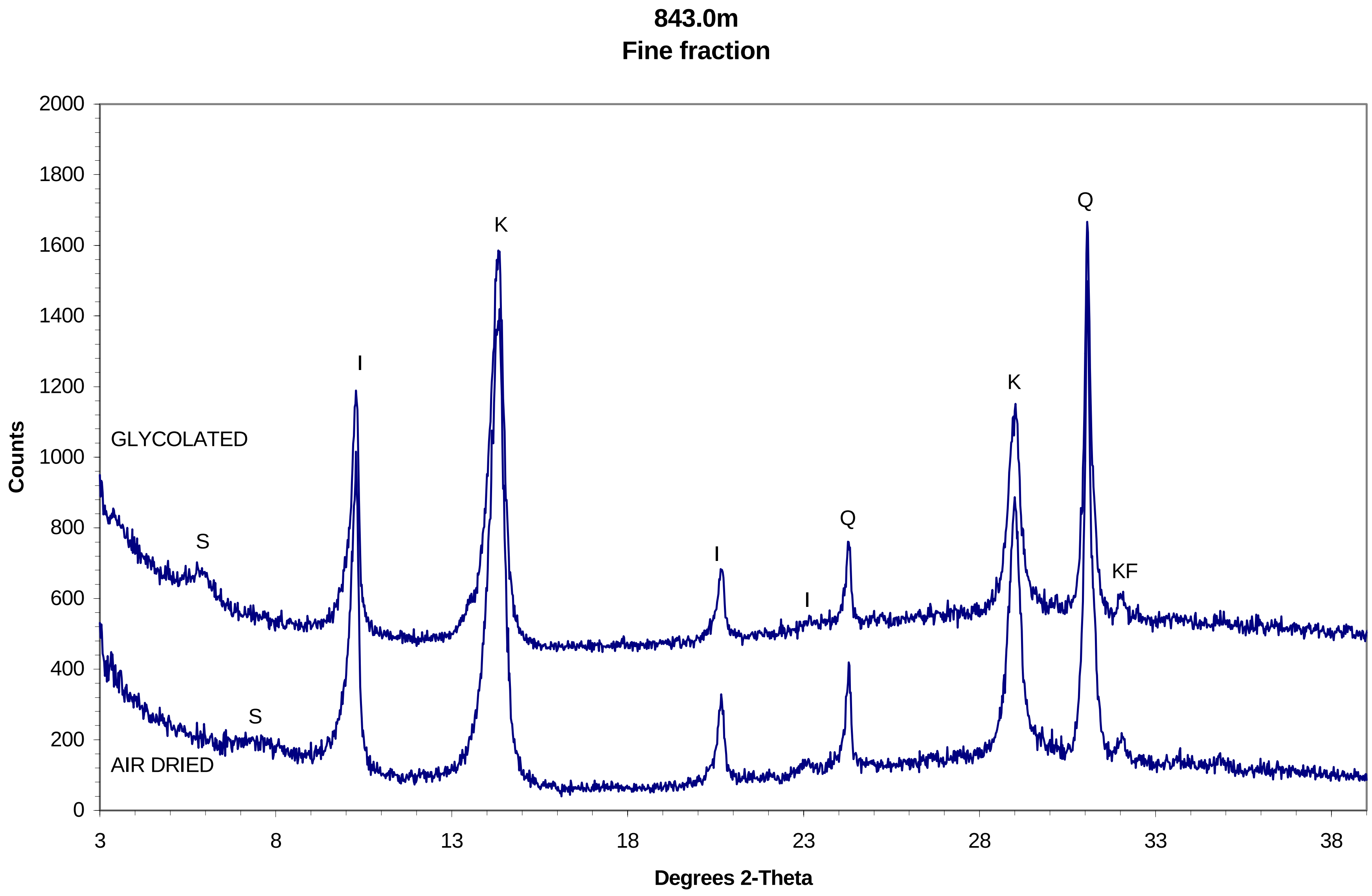
843.0m
Fine fraction
Counts
Degrees 2-Theta
GLYCOLATED
AIR DRIED
S
I
K
Q
KF
0
200
400
600
800
1000
1200
1400
1600
1800
2000
3
8
13
18
23
28
33
38

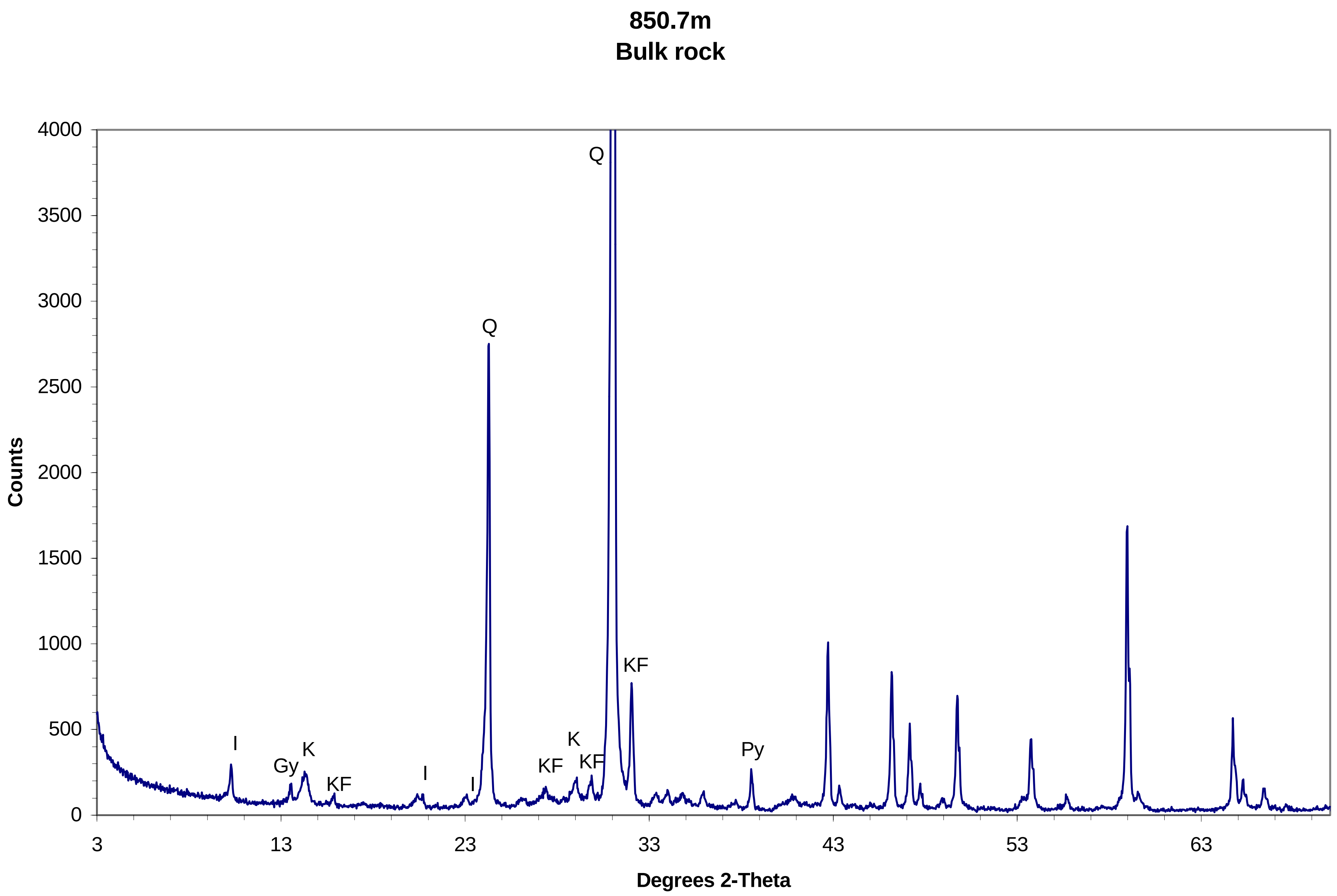
850.7m
Bulk rock
Counts
4000
3500
3000
2500
2000
1500
1000
500
0
3
13
23
33
43
53
63
Degrees 2-Theta
Q
Q
KF
I
Gy
K
KF
I
I
KF
K
KF
Py

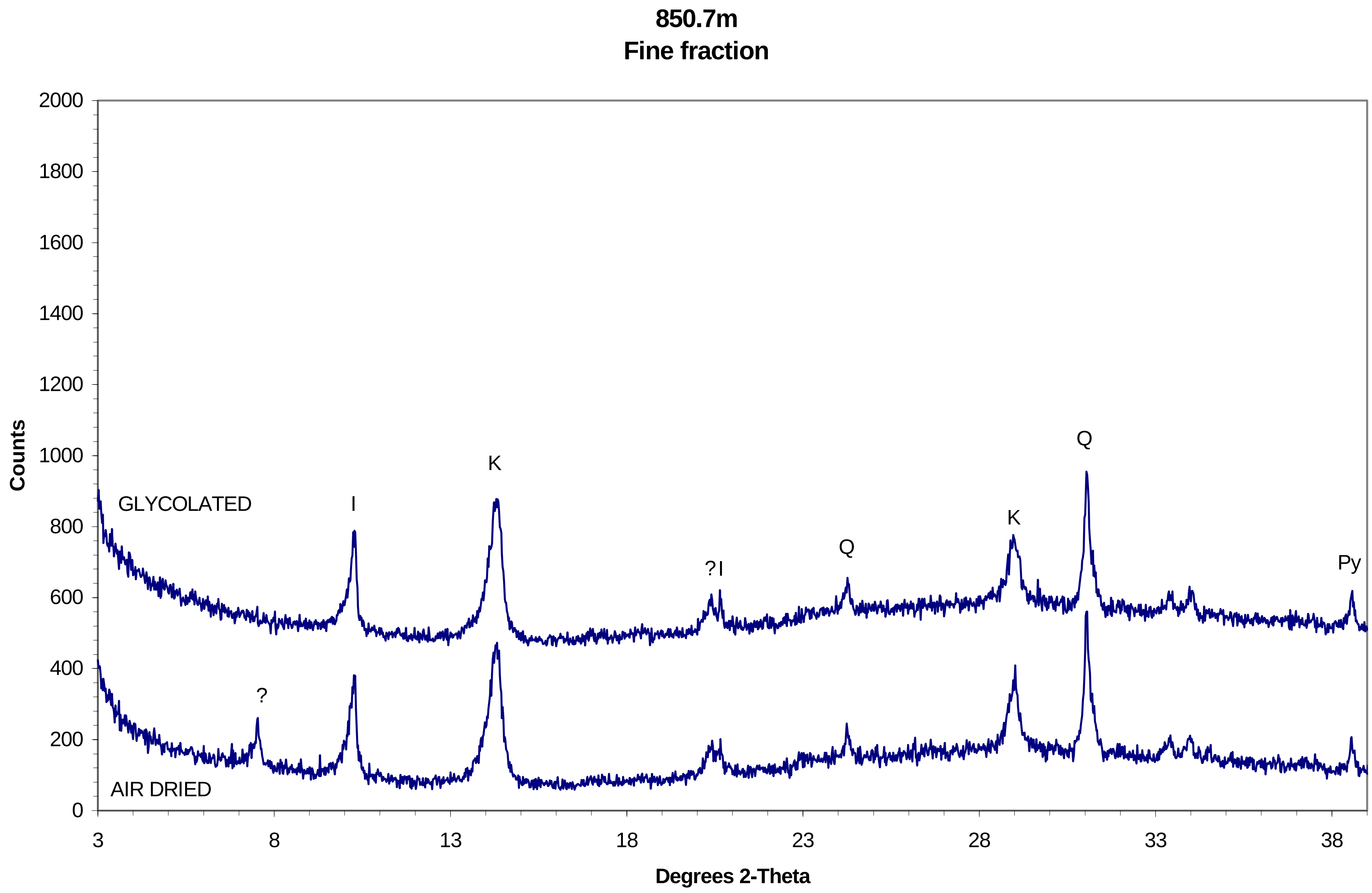
850.7m
Fine fraction
Counts
2000
1800
1600
1400
1200
1000
800
600
400
200
0
GLYCOLATED
AIR DRIED
I
K
?I
Q
K
Q
Py
?
3
8
13
18
23
28
33
38
Degrees 2-Theta

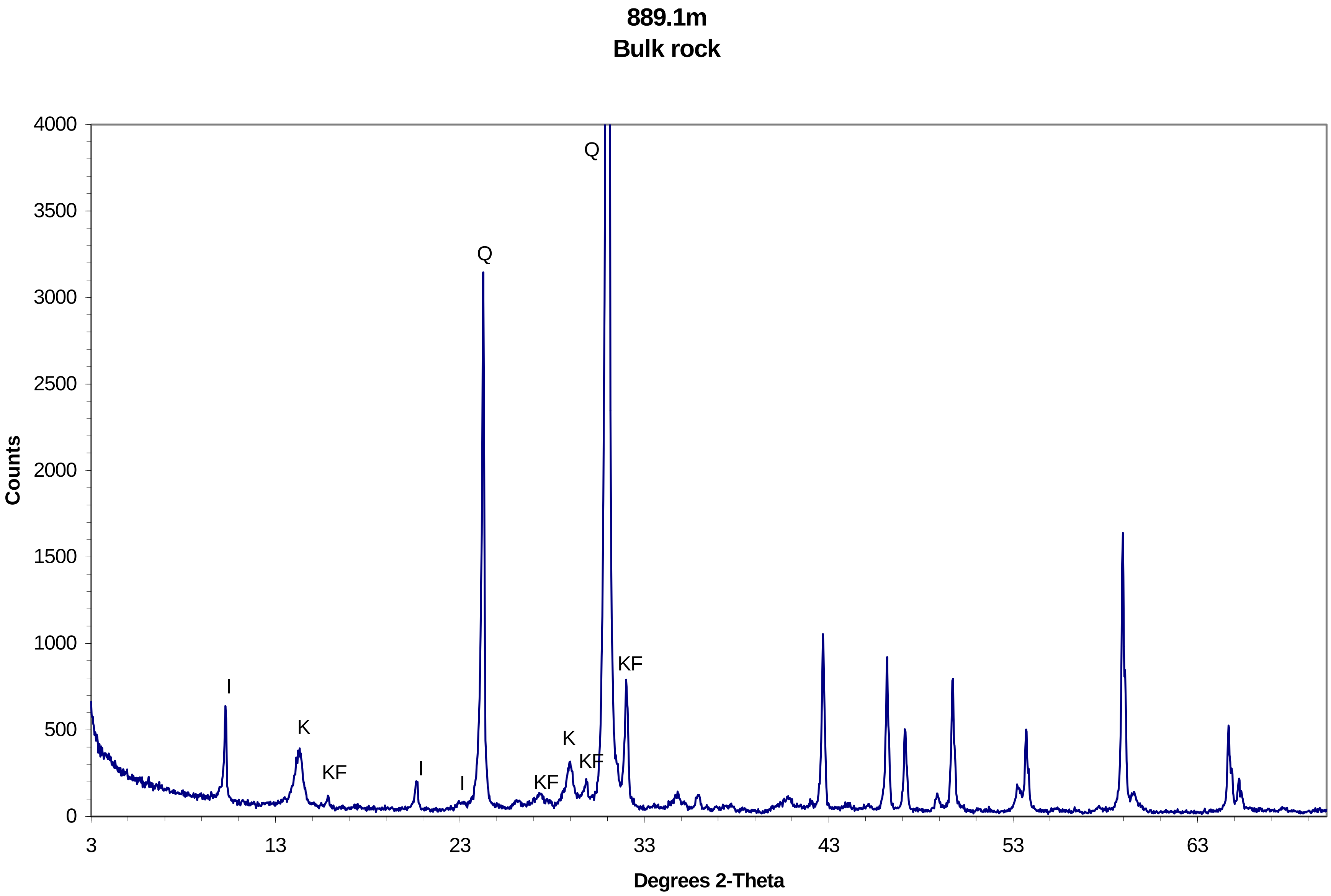
889.1m
Bulk rock
Counts
4000
3500
3000
2500
2000
1500
1000
500
0
3
13
23
33
43
53
63
Degrees 2-Theta
Q
Q
KF
I
K
KF
I
I
KF
K
KF

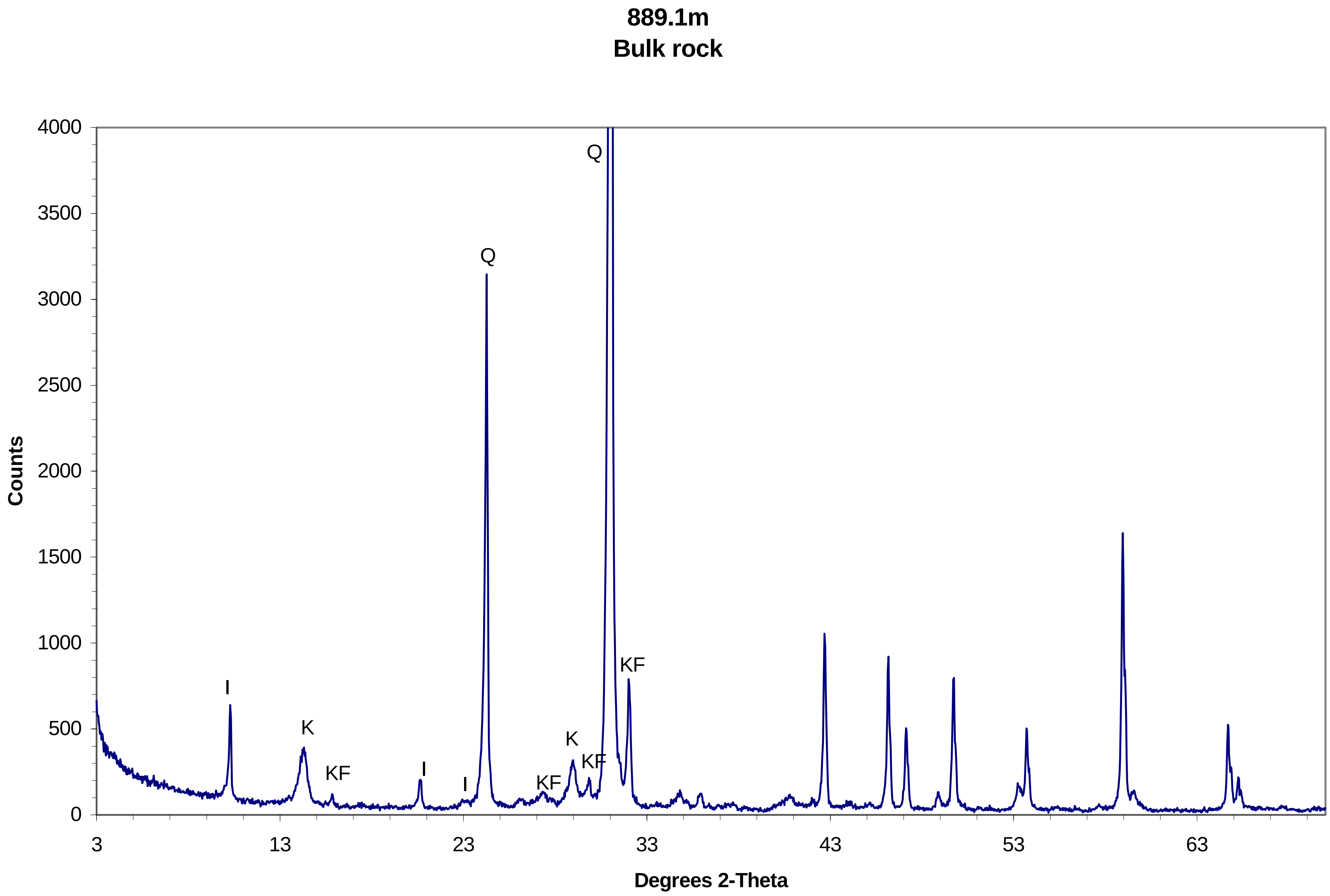
889.1m
Bulk rock
Counts
Degrees 2-Theta
4000
3500
3000
2500
2000
1500
1000
500
0
3
13
23
33
43
53
63
Q
Q
KF
I
K
KF
I
I
KF
K
KF

APPENDIX 2

PHOTOMICROGRAPHS

PLATE 1 817.1m

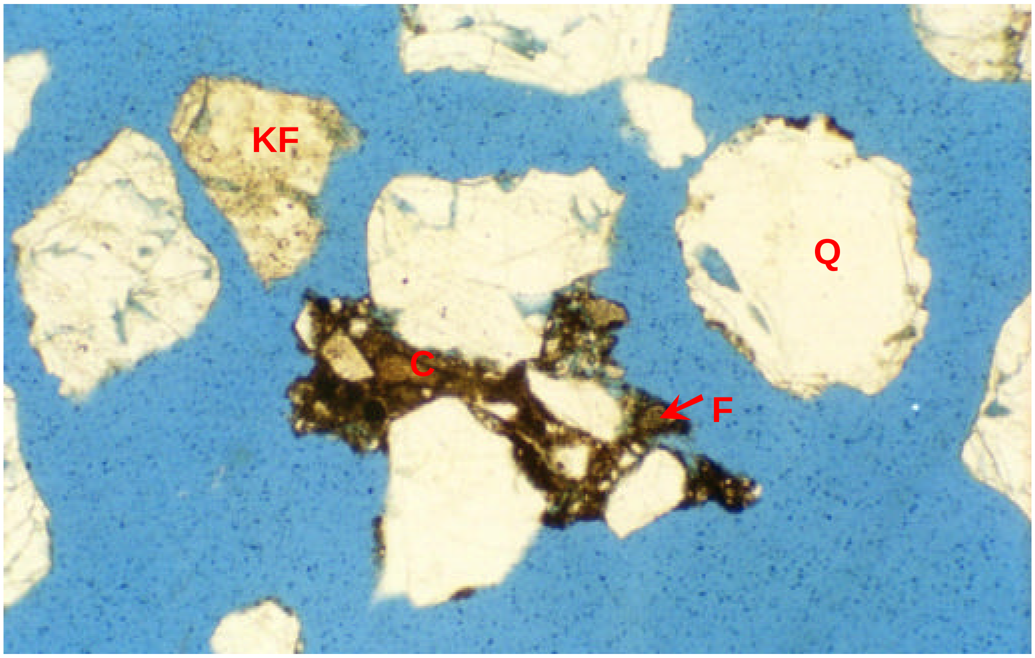

FIGURE 1 Plane polarised light
FIGURE 2 Crossed polarisers

0.4mm

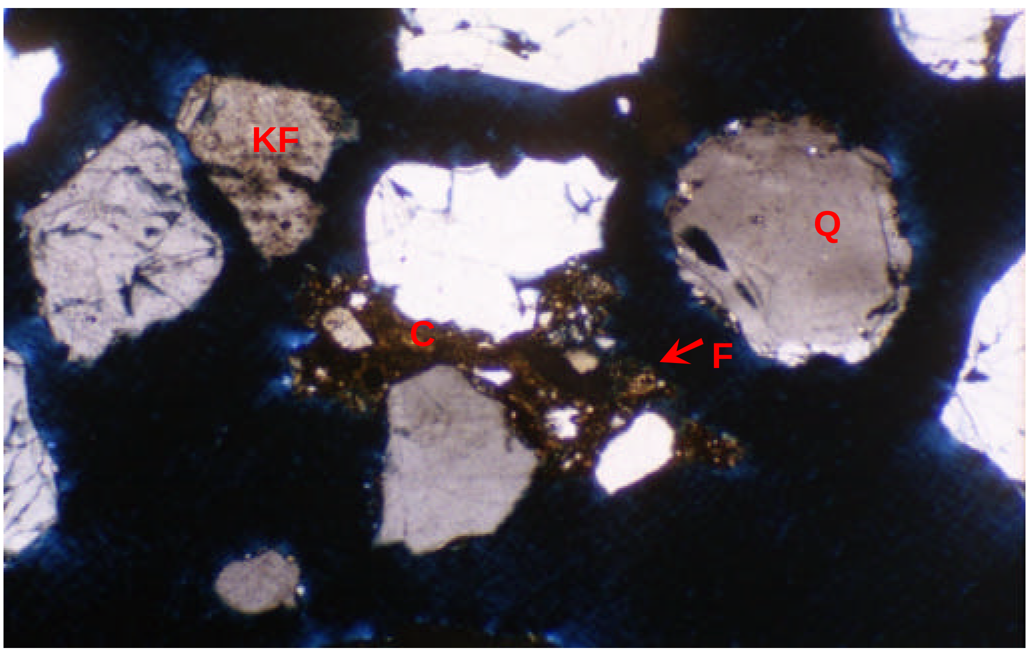

This sample is composed mainly of loose, coarse sand- to granule-sized quartz (Q) and minor K-feldspar (KF) grains, and also includes small fragments of argillaceous sandstone in which intergranular areas are occupied by clay matrix (C). A foram test (F) is included within the marked clay matrix.

PLATE 2   817.1m cont.

FIGURE 1

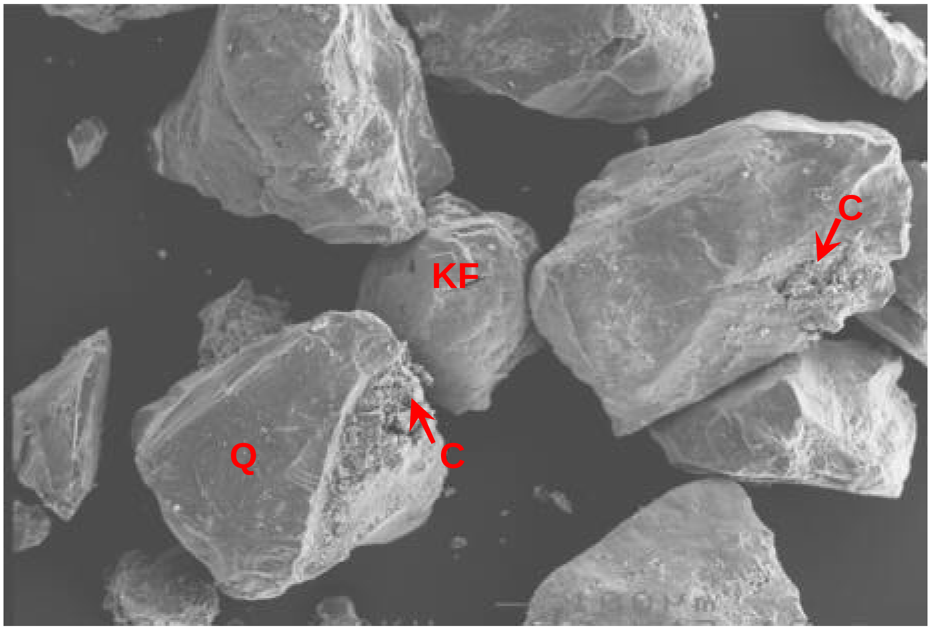

100mm

SEM micrograph showing typical loose grains of quartz (Q) and K-feldspar (KF). The presence of detrital clay (C) on grain surfaces indicates that grains are derived from argillaceous lithologies.

FIGURE 2

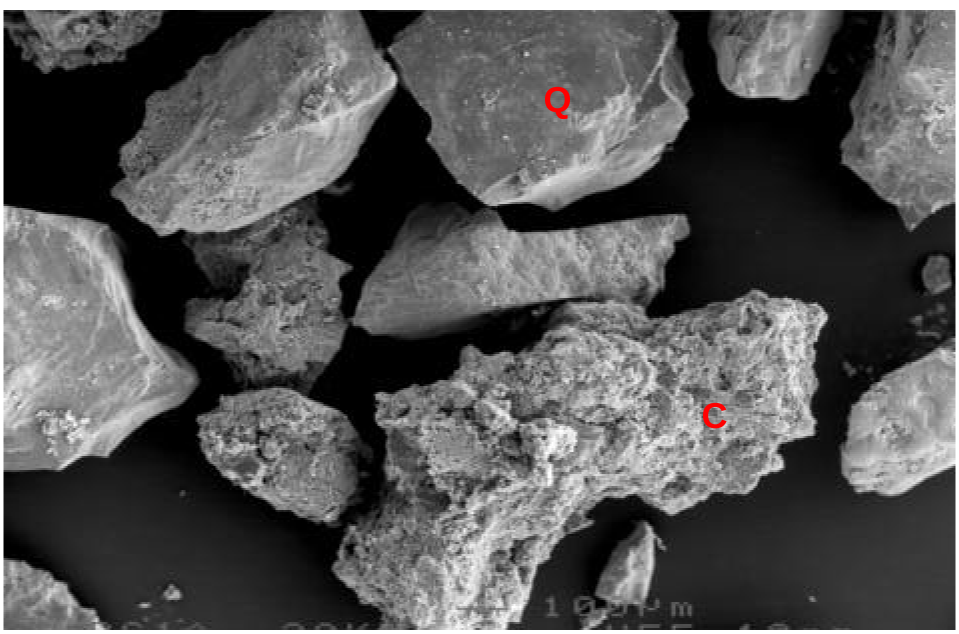

100mm

In addition to loose quartz grains (Q), the sample includes mudrock fragments that are composed mainly of clay (C).

PLATE 3 818.7m

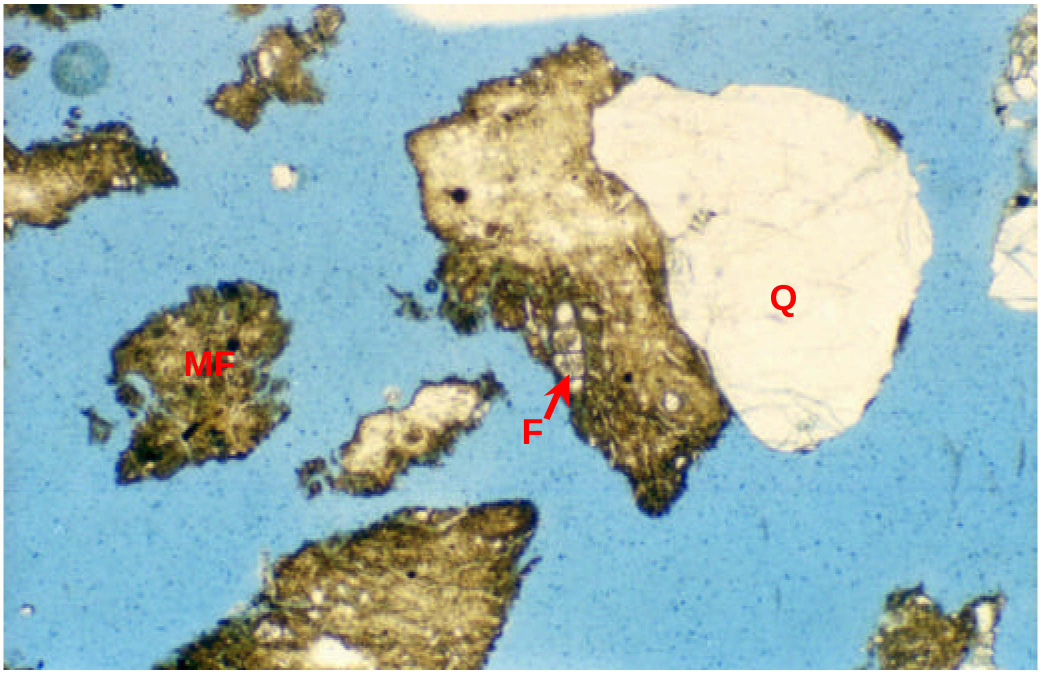

FIGURE 1 Plane polarised light
FIGURE 2 Crossed polarisers

0.4mm

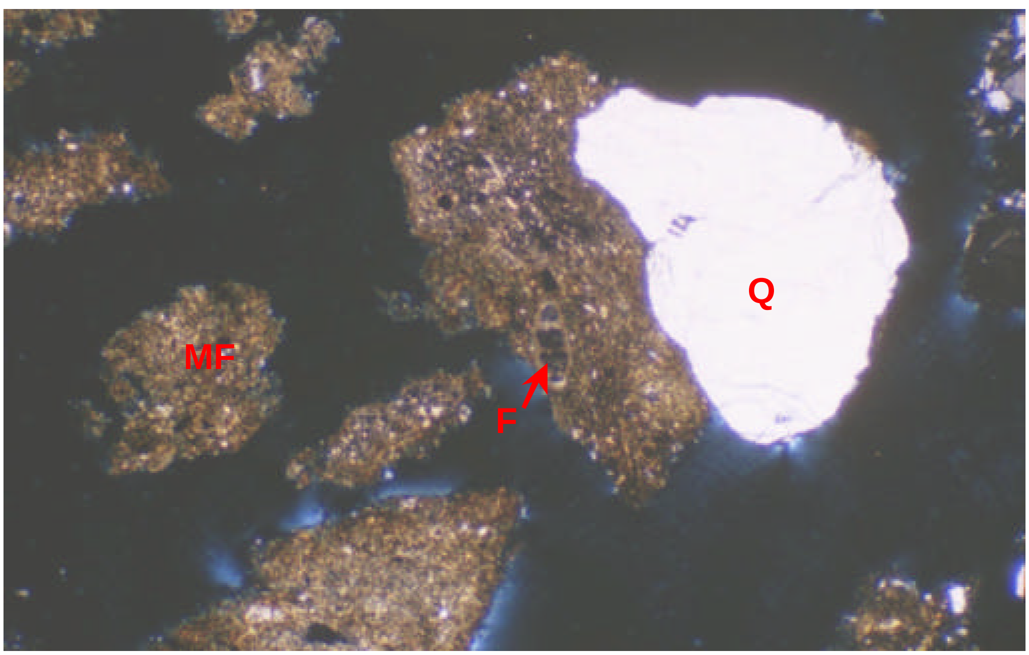

Like the previous sample, this sample includes mudrock fragments (MF) that locally contain coarse to very coarse sand-sized quartz grains (Q). Many loose quartz grains that occur in the sample appear to be derived from argillaceous lithologies. A foram test (F) is also marked.

PLATE 4 818.7m cont.

FIGURE 1

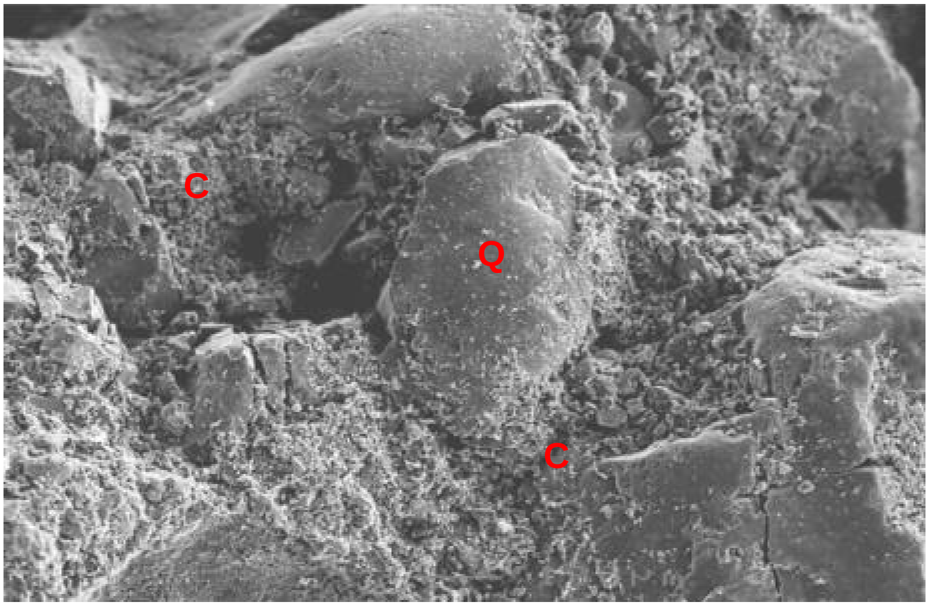

100mm

Impact-damaged, argillaceous sandstone fragment in which all intergranular areas between coarse quartz grains (Q) are occupied by detrital clay (C).

FIGURE 2

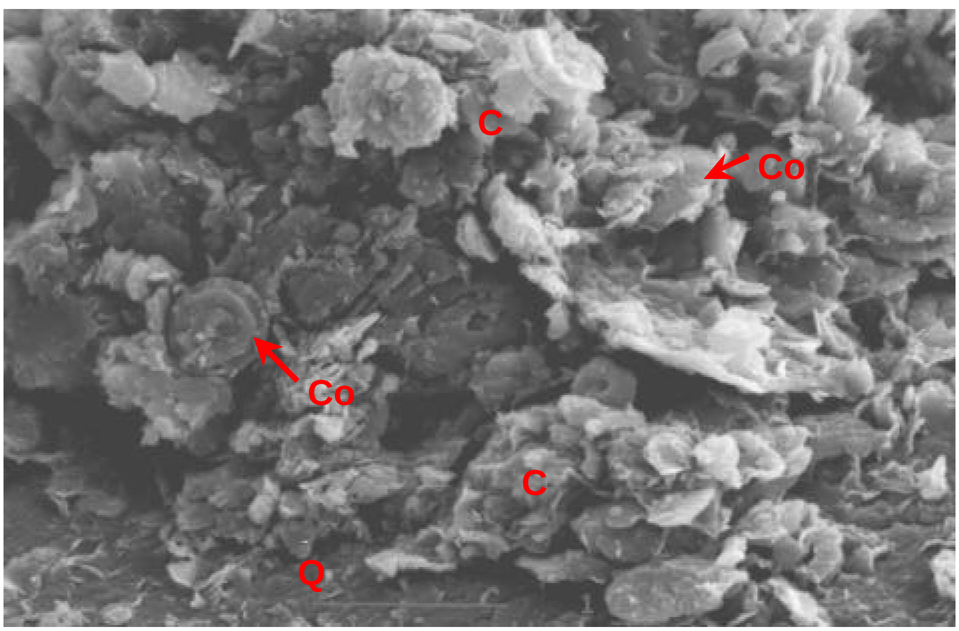

10mm

The surface of a loose, coarse sand-sized quartz grain (Q) is partly covered by detrital clay (C), indicating that the quartz grain is derived from an argillaceous sandstone or sandy mudrock. Coccoliths (Co) are associated with the clay.

PLATE 5 822.0m

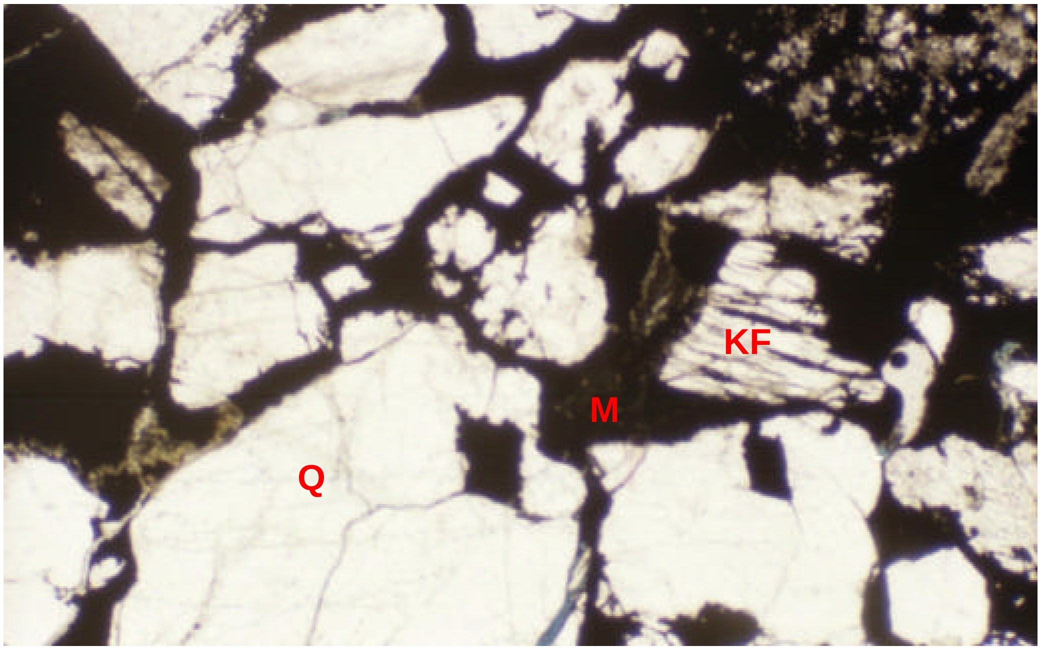

FIGURE 1 Plane polarised light
FIGURE 2 Crossed polarisers

0.4mm

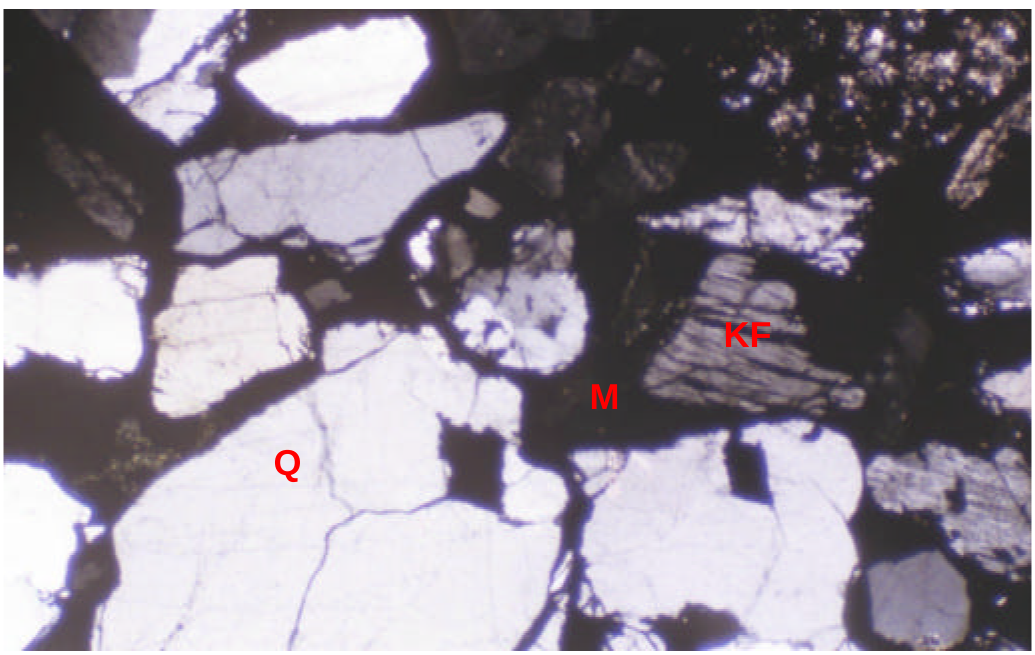

All intergranular areas in this impact-damaged subarkose are filled by early-diagenetic marcasite (FeS_2) cement (M). Framework grains, which consist almost entirely of granitic quartz (Q) and K-feldspar (KF), are commonly supported by marcasite cement.

PLATE 6 822.0m cont.

FIGURE 1

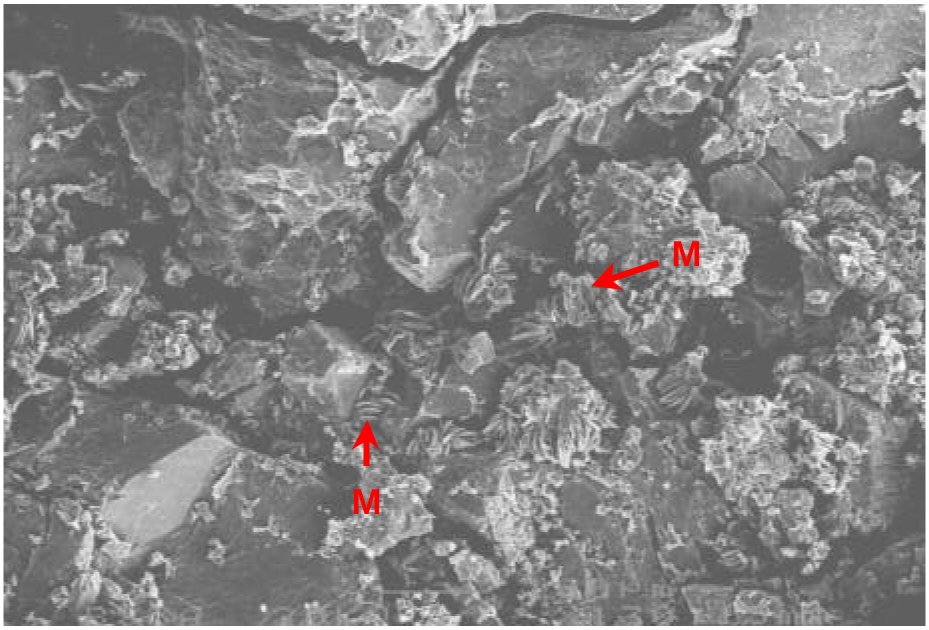

100μm

SEM micrograph showing artificially-fractured sandstone in which intergranular areas are occupied by marcasite (FeS_2) cement (M).

FIGURE 2

10μm

Detail of typical pore-filling marcasite cement (M), the presence of which would result in very low permeability.

PLATE 7 835.7m

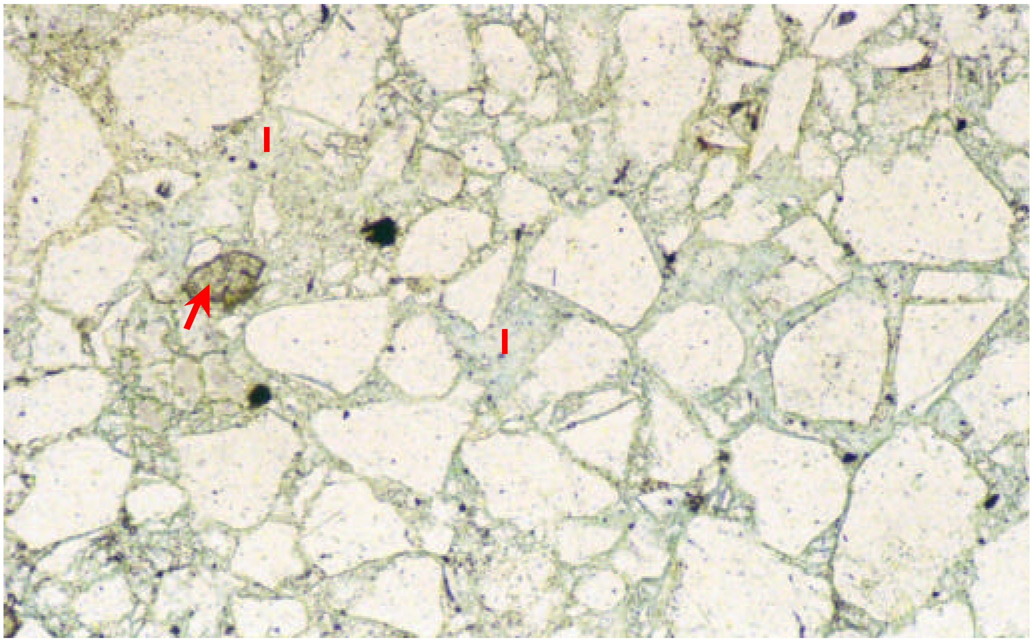

FIGURE 1 Plane polarised light
FIGURE 2 Crossed polarisers

0.2mm

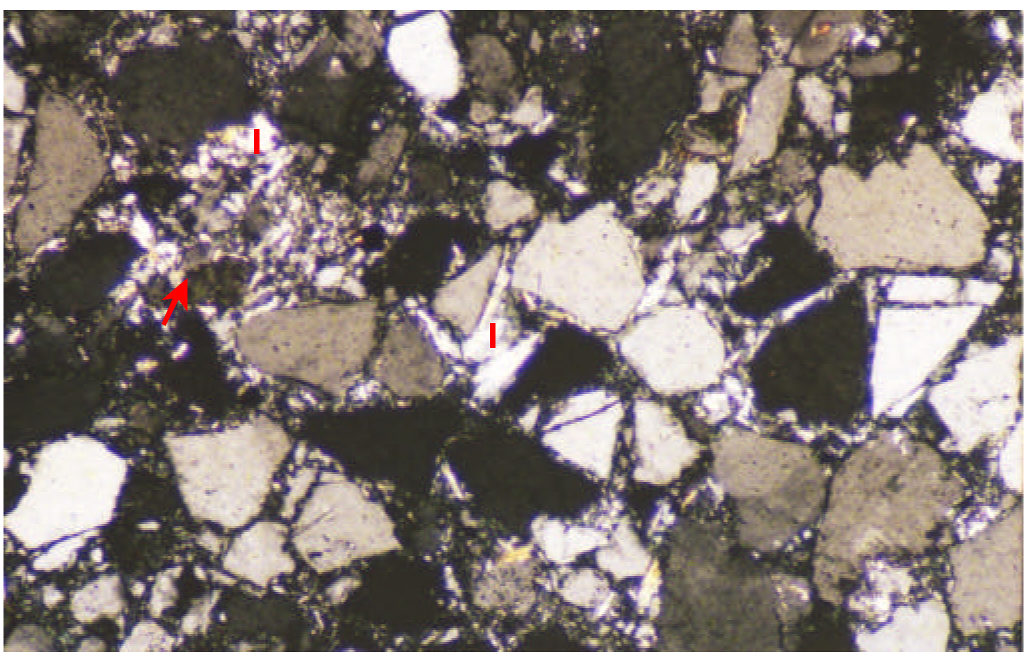

Fine grained subarkose in which all intergranular areas are filled by illitic clay pseudomatrix (I) that has formed by alteration of micaceous grains. The clay is highly microporous as shown by its blue hue. The sandstone contains widely scattered grains of monazite (arrow), the presence of which most likely accounts for the sandstone having a high gamma ray value.

PLATE 8 835.7m cont.

FIGURE 1

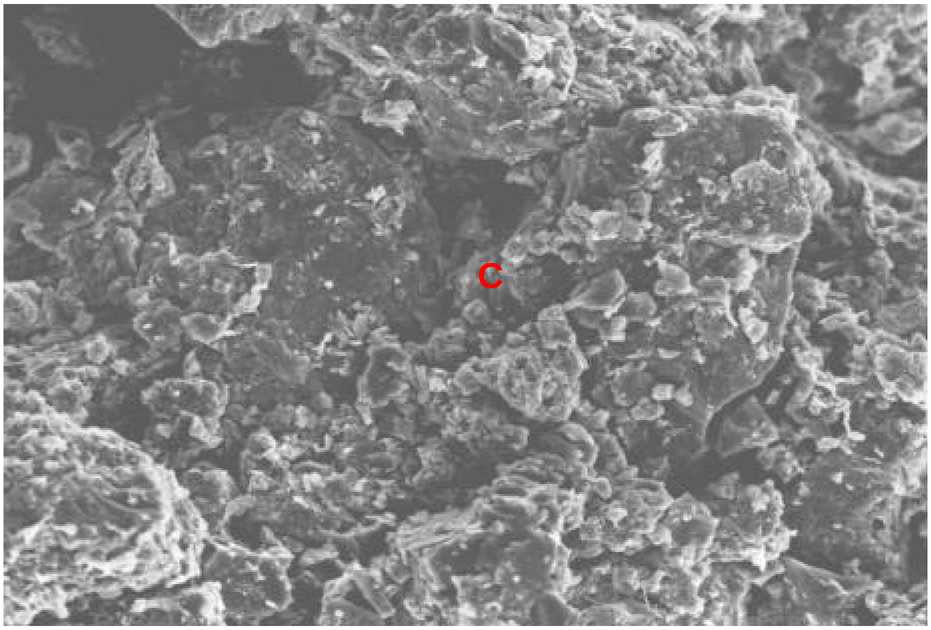

10mm

SEM micrograph showing a representative area in which all intergranular spaces are filled by authigenic illitic and kaolinitic clay (C).

FIGURE 2

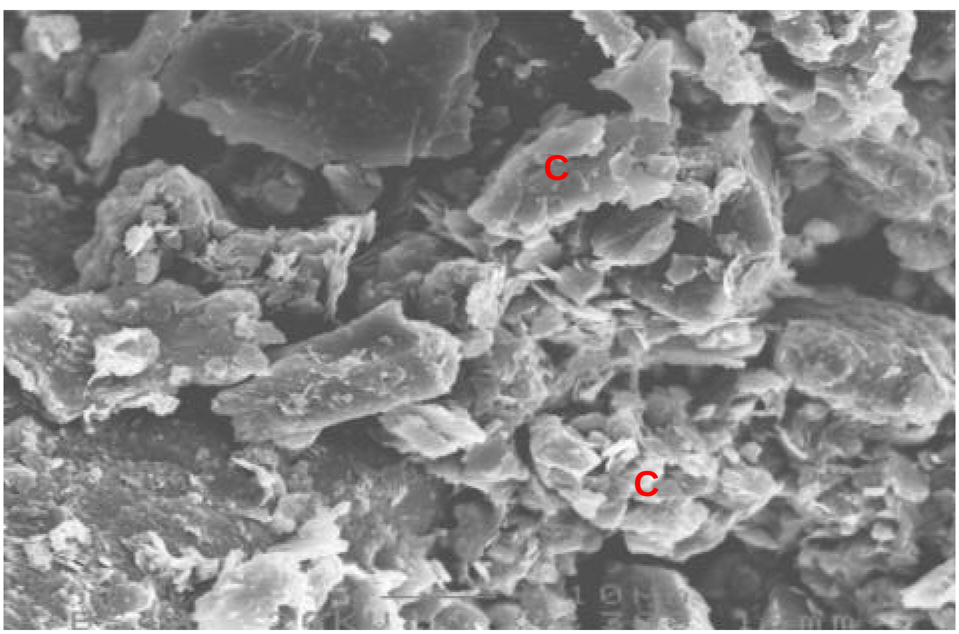

10mm

Detail of pore-filling clay (C) that has formed by mica alteration. The sandstone is totally microporous due to the presence of such clay in all intergranular spaces.

PLATE 9 837.9m

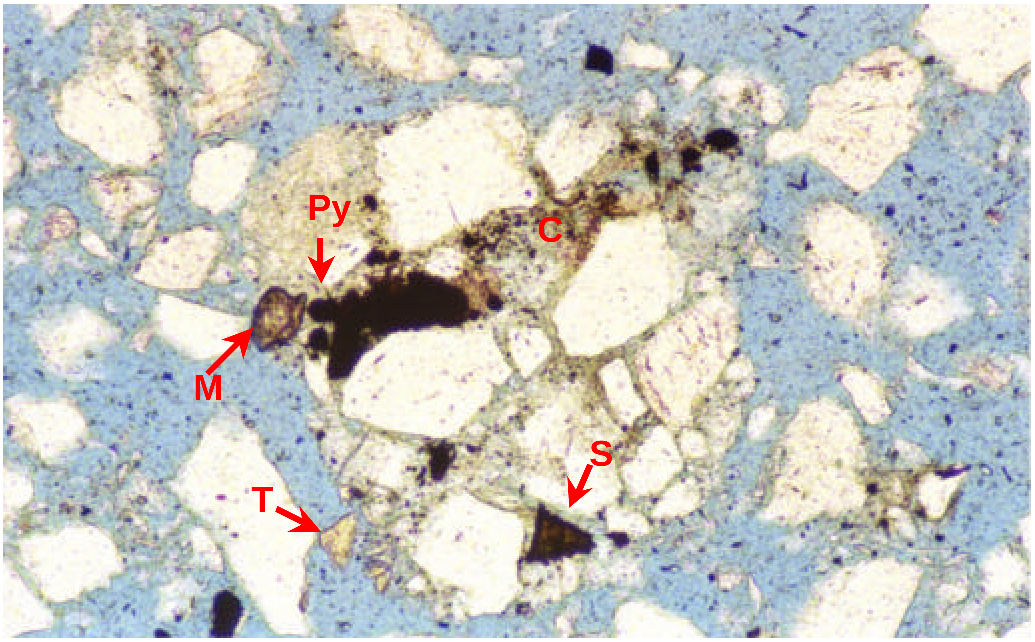

FIGURE 1 Plane polarised light
FIGURE 2 Crossed polarisers

0.2mm

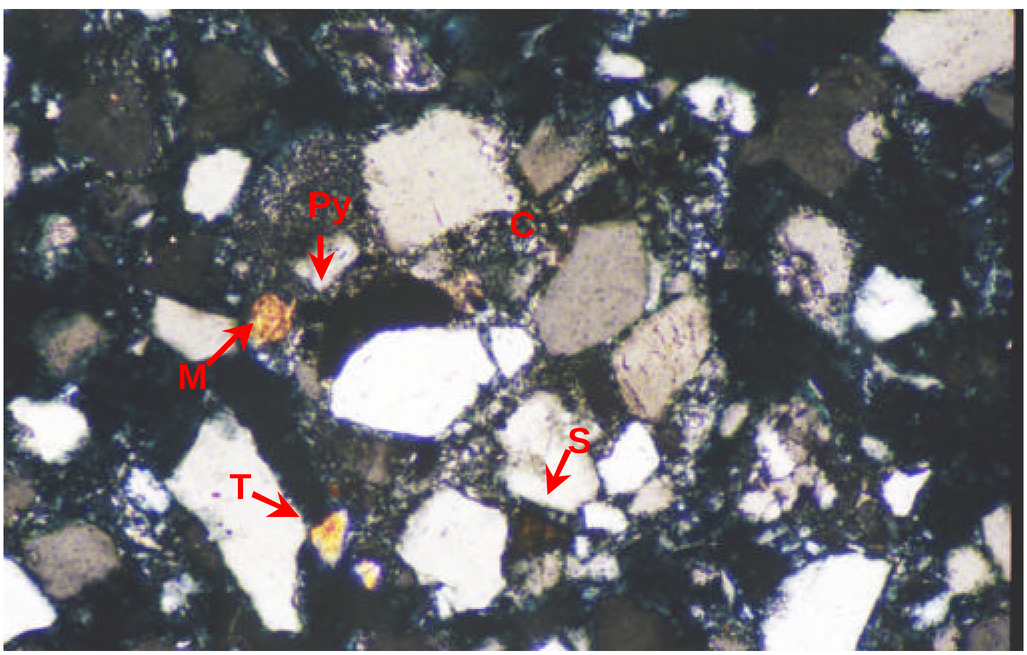

This sample consists mainly of loose grains and also includes intact sandstone fragments in which all intergranular areas are filled by authigenic clay (C). Fine pyrite (Py) is locally associated with authigenic clay. Heavy minerals include monazite (M), sphene (S) and tourmaline (T).

PLATE 10 837.9m cont.

FIGURE 1

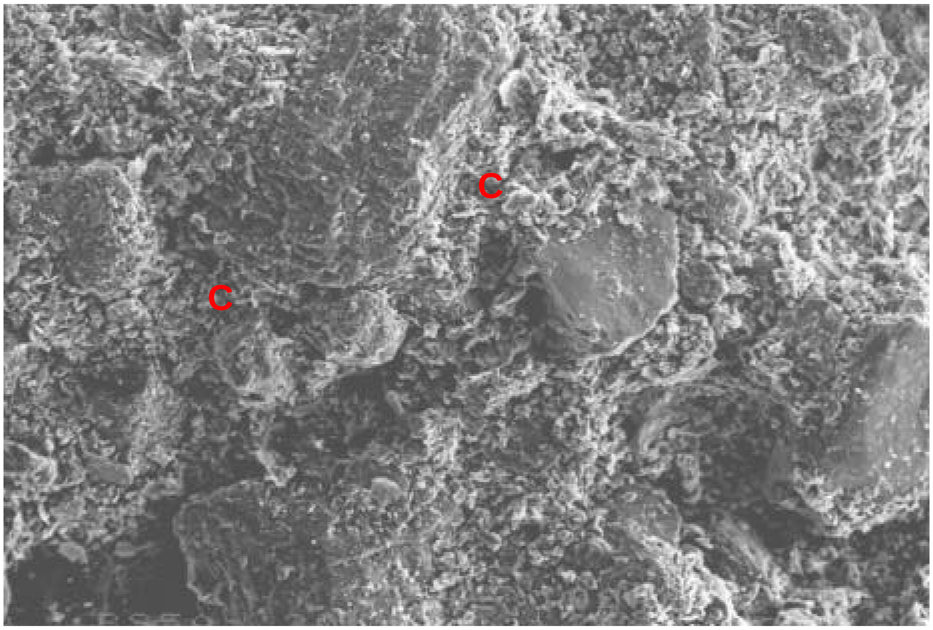

100μm

Representative intact sandstone fragment in which all intergranular areas are filled by authigenic clay (C) that is the altered and dispersed remnant of mica.

FIGURE 2

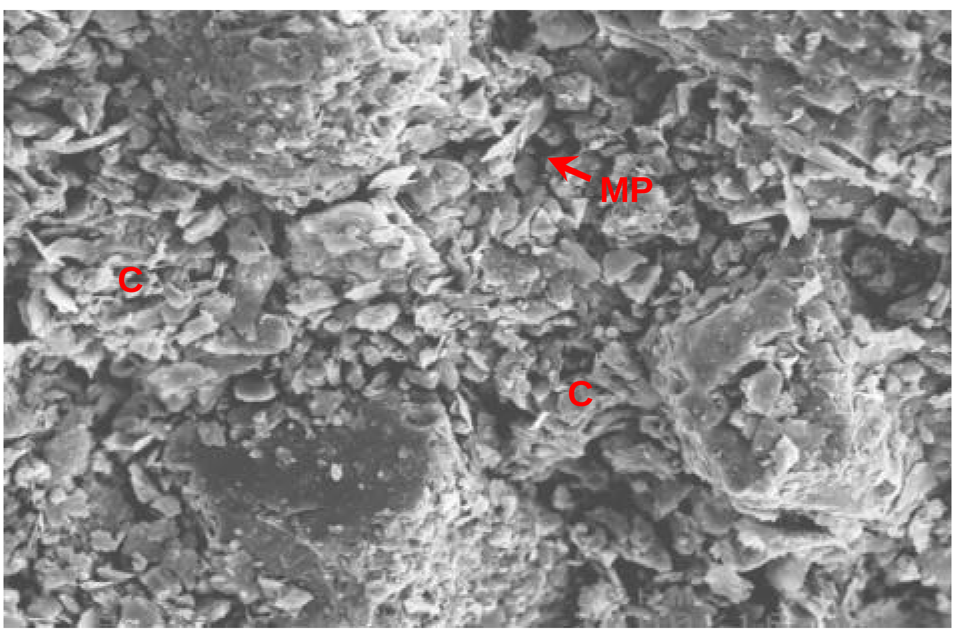

10μm

Detail of typical pore-filling illitic/kaolinitic authigenic clay (C), the presence of which would result in low permeability. Abundant microporosity (MP) is associated with the clay.

PLATE 11 843.0m

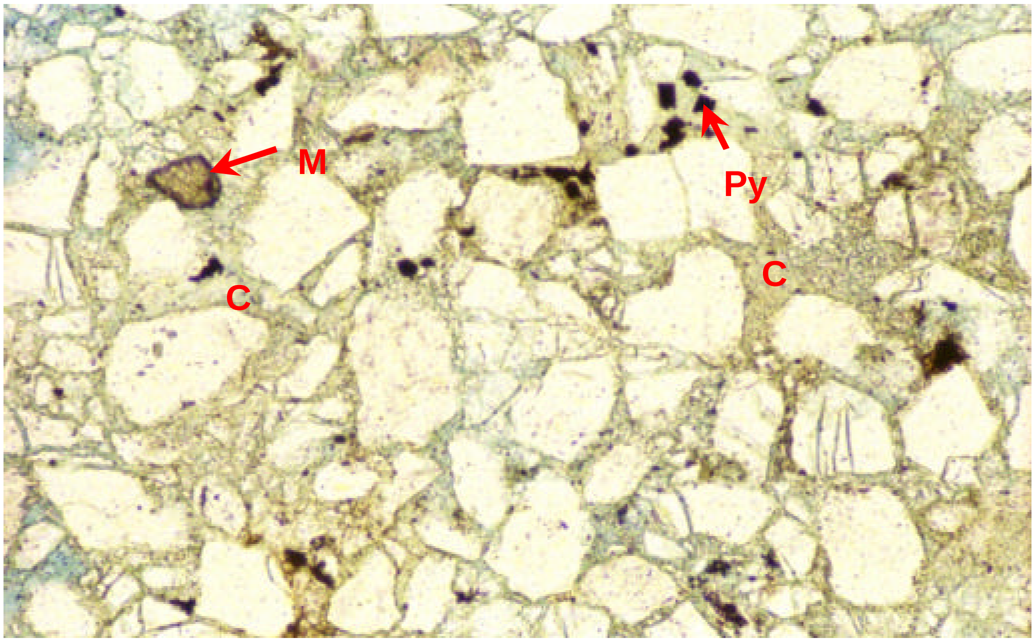

FIGURE 1 Plane polarised light
FIGURE 2 Crossed polarisers

0.2mm

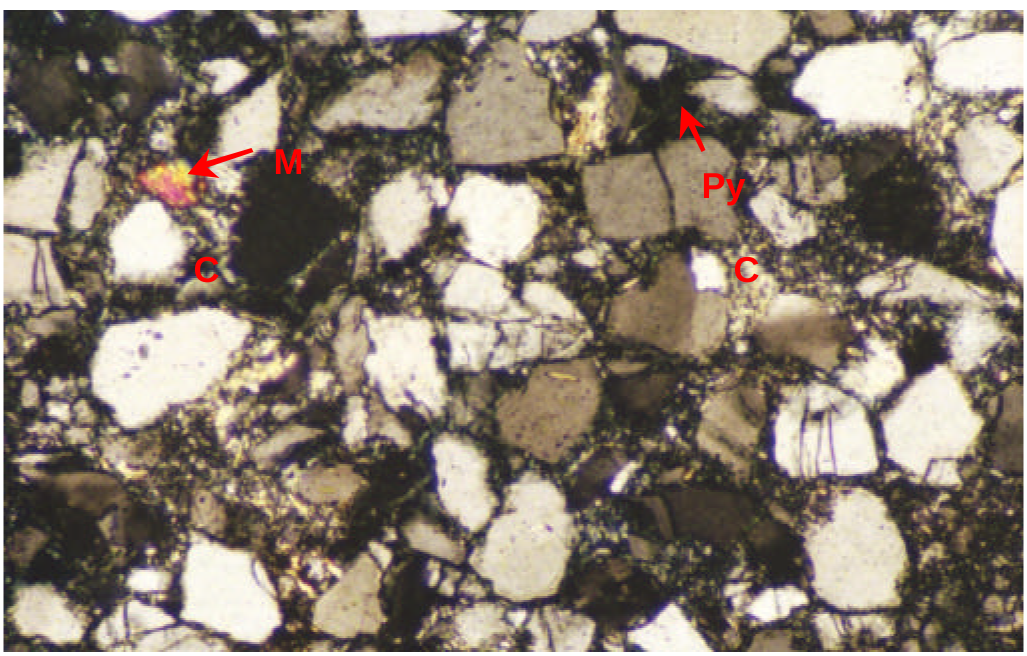

Microporous, fine grained subarkose that lacks intergranular porosity due to pore filling by illitic/kaolinitic clay pseudomatrix (C) that has formed by alteration of micaceous grains. Fine pyrite (Py) occurs where biotite has altered to kaolinite. The sandstone contains widely scattered monazite grains (M).

PLATE 12 843.0m cont.

FIGURE 1

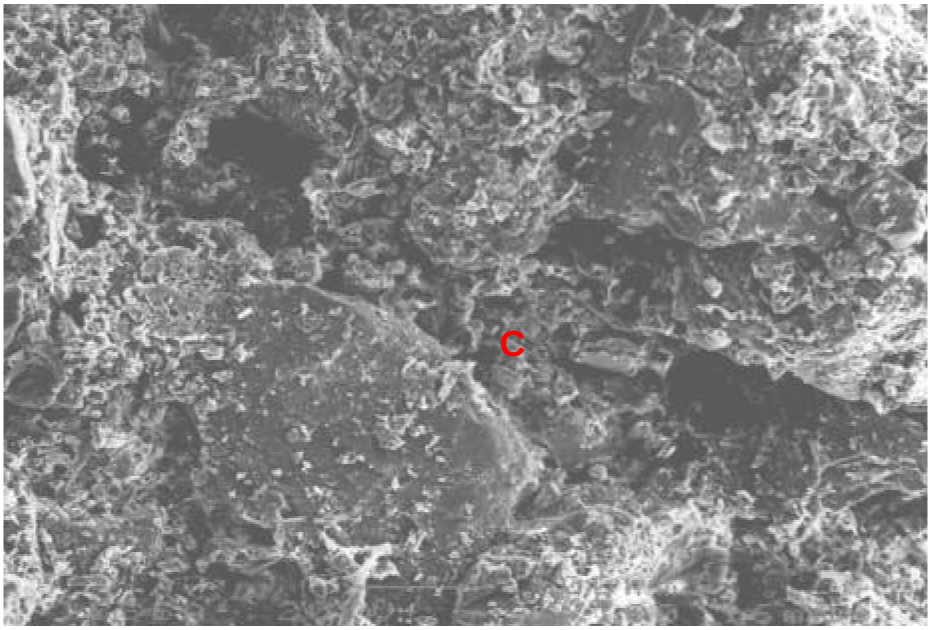

100mm

This sandstone is totally microporous due to all intergranular areas being filled by authigenic clay (C).

FIGURE 2

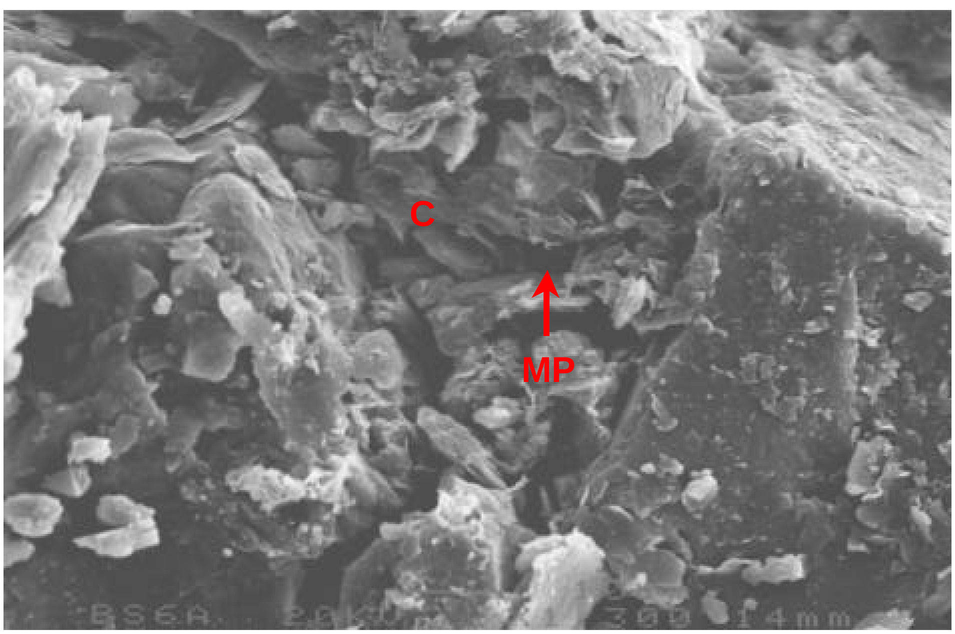

10mm

Detail of typical authigenic clay (C) and associated microporosity (MP) that are the result of mica alteration.

PLATE 13 850.7m

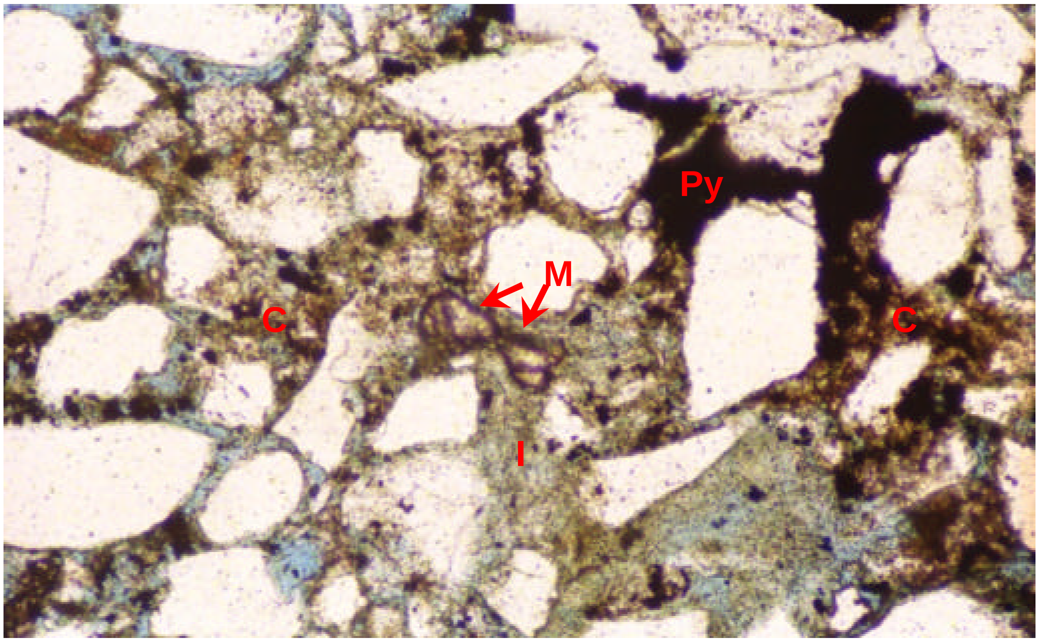

FIGURE 1 Plane polarised light
FIGURE 2 Crossed polarisers

0.2mm

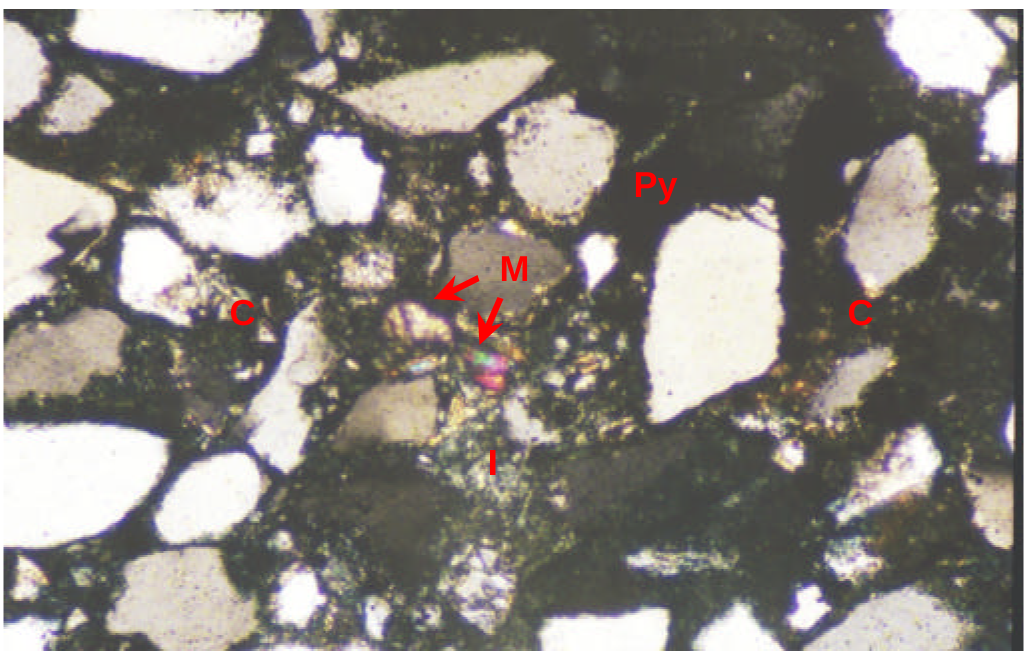

Low permeability sandstone in which all intergranular areas are filled by detrital clay (C), authigenic illite (I), and patchy pyrite cement (Py). Monazite grains (M) are not as common as in the previous fine grained sandstones. Porosity (blue) is artificial.

PLATE 14 850.7m cont.

FIGURE 1

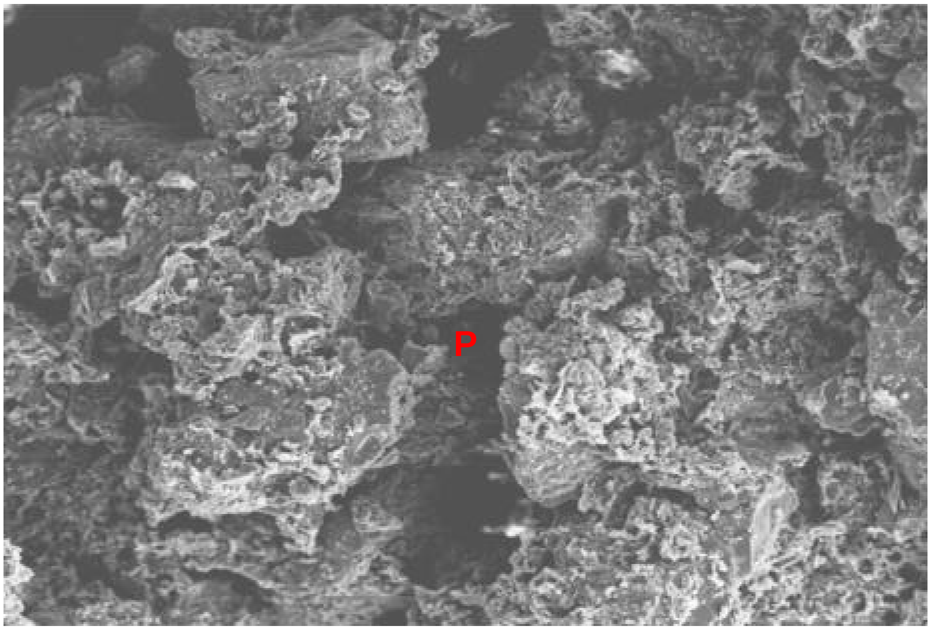

100mm

Rare intergranular pores (P) that are preserved in a slightly less argillaceous part of the sample would not be conducive to permeability.

FIGURE 2

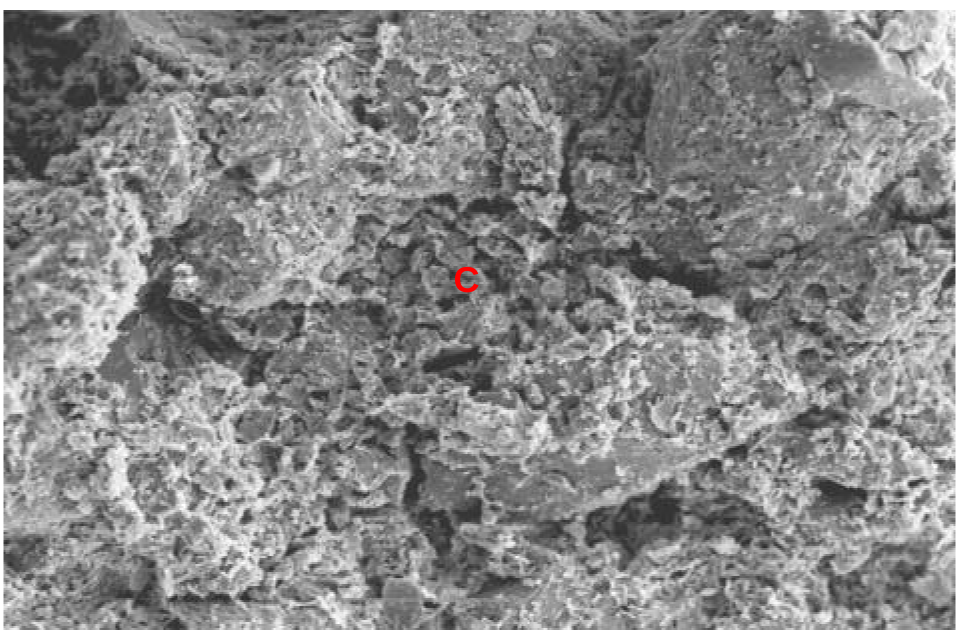

100mm

Throughout most of the sandstone, intergranular pores are totally filled by detrital clay (C) and pyrite. Consequently, permeability would be very low.

PLATE 15 889.1m

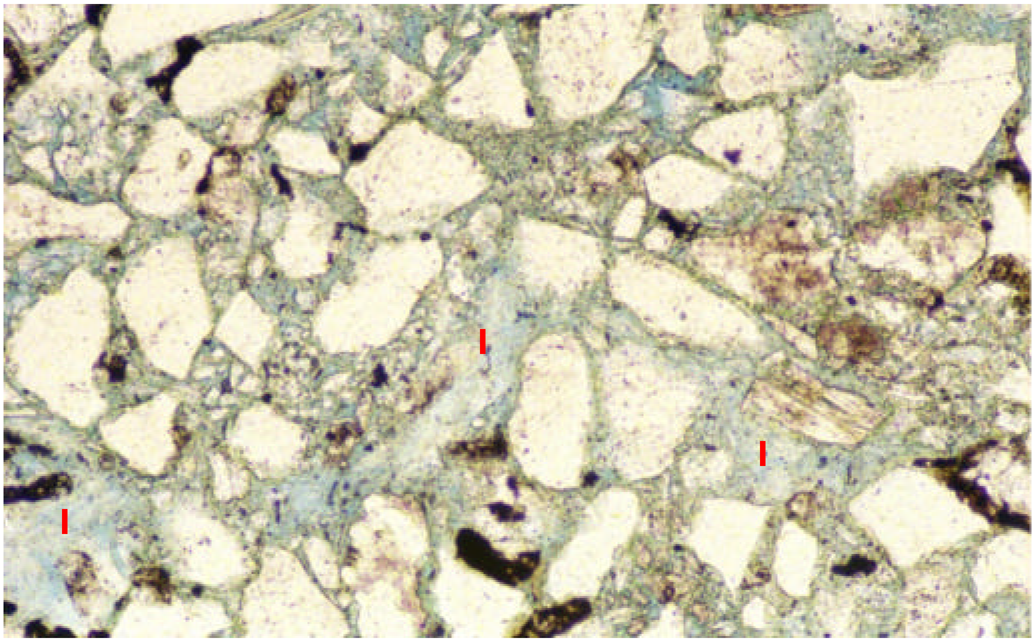

FIGURE 1   Plane polarised light
FIGURE 2   Crossed polarisers

0.2mm

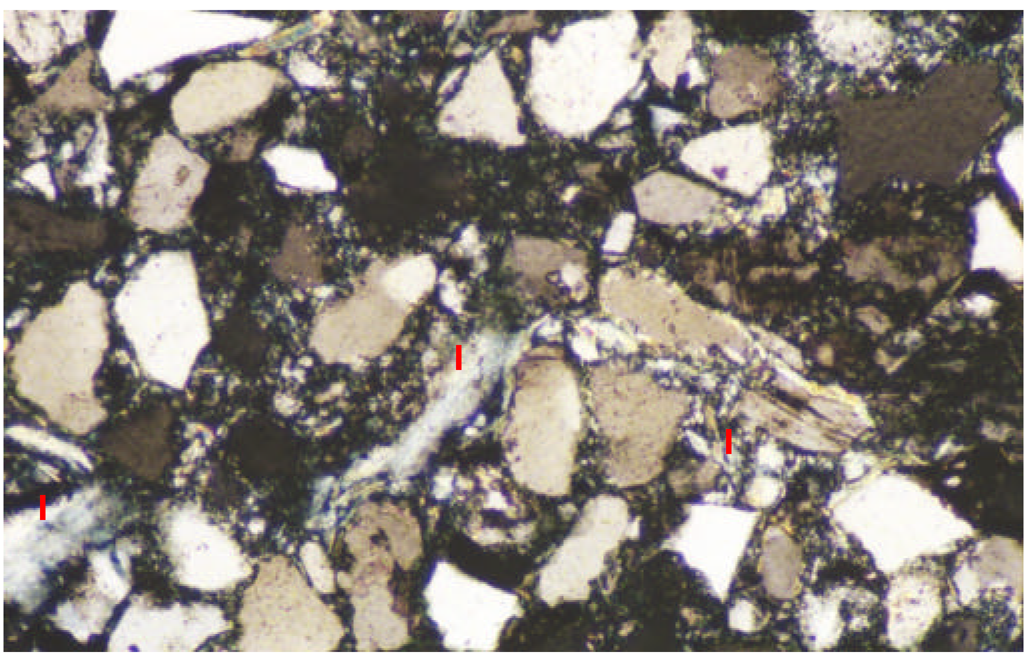

Abundant pore-filling illitic clay pseudomatrix (I) is the result of alteration and compactional deformation/dispersion of micaceous grains, which were originally abundant in the sample. Little intergranular porosity remains due to extensive authigenic clay formation and compaction. The clay has a blue hue on account of being sufficiently microporous for impregnation by epoxy resin.

PLATE 16 889.1m cont.

FIGURE 1

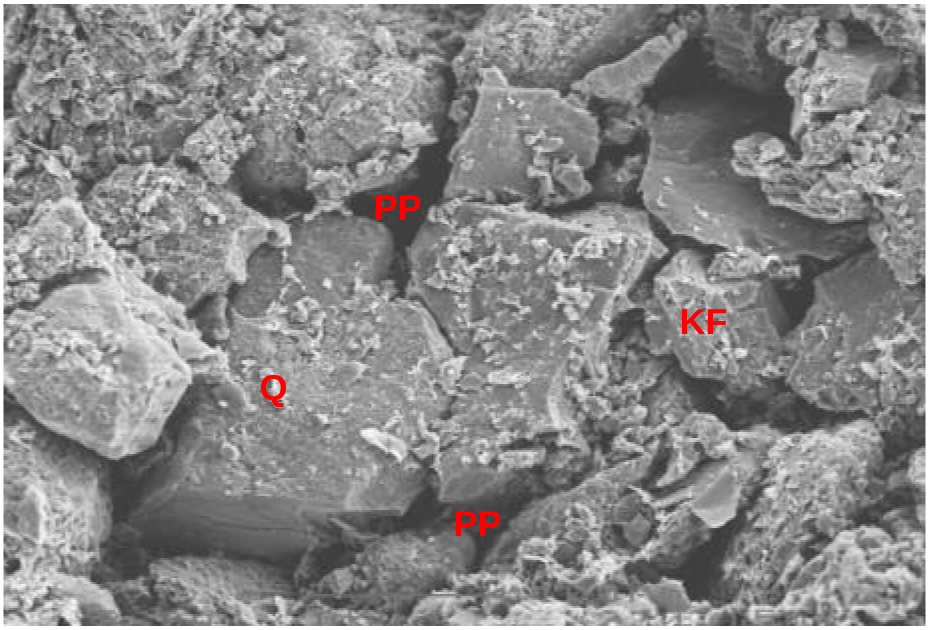

100μm

This SEM micrograph shows a relatively clean area where primary intergranular pores (PP) are preserved between loosely packed and uncemented quartz (Q) and K-feldspar (KF) framework grains. Primary pores have a restricted distribution in the sandstone, and thus would not be conducive to permeability.

FIGURE 2

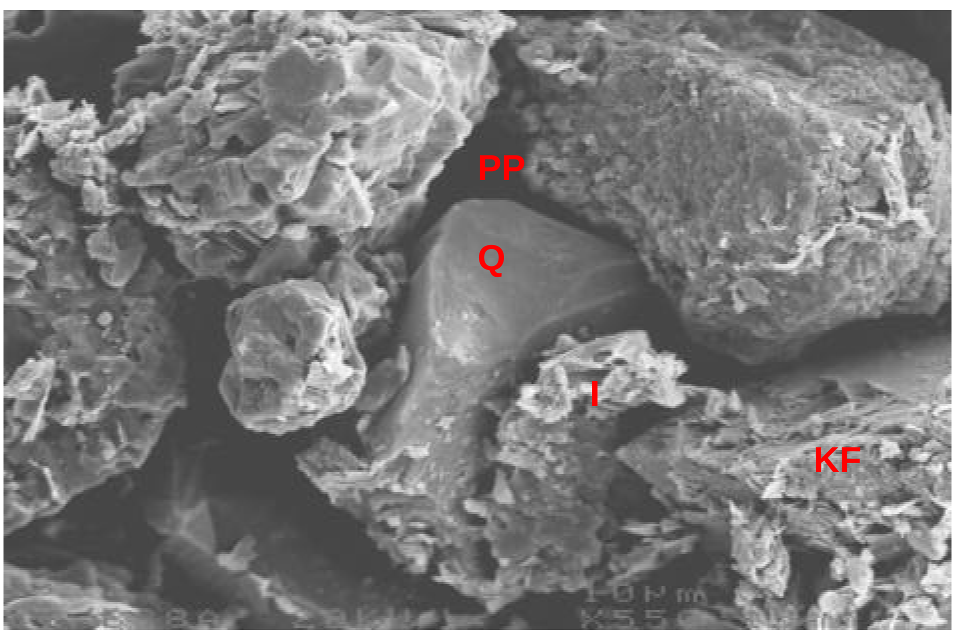

10μm

Detail of typical primary intergranular pores (PP) that are preserved between poorly compacted quartz (Q) and K-feldspar (KF) framework grains. Illitic clay (I) partly occupies one pore.